

# Gene Expression by Mouse Inner Ear Hair Cells during Development

**Déborah I. Scheffer,<sup>1,2\*</sup> Jun Shen,<sup>1,3\*</sup> David P. Corey,<sup>1</sup> and Zheng-Yi Chen<sup>2</sup>**

<sup>1</sup>Department of Neurobiology and Howard Hughes Medical Institute, Harvard Medical School, Boston, Massachusetts 02115, <sup>2</sup>Department of Otolaryngology, Harvard Medical School and Massachusetts Eye and Ear, Boston, Massachusetts 02114, and <sup>3</sup>Department of Pathology, Brigham and Women's Hospital, Harvard Medical School, Boston, Massachusetts 02115

Hair cells of the inner ear are essential for hearing and balance. As a consequence, pathogenic variants in genes specifically expressed in hair cells often cause hereditary deafness. Hair cells are few in number and not easily isolated from the adjacent supporting cells, so the biochemistry and molecular biology of hair cells can be difficult to study. To study gene expression in hair cells, we developed a protocol for hair cell isolation by FACS. With nearly pure hair cells and surrounding cells, from cochlea and utricle and from E16 to P7, we performed a comprehensive cell type-specific RNA-Seq study of gene expression during mouse inner ear development. Expression profiling revealed new hair cell genes with distinct expression patterns: some are specific for vestibular hair cells, others for cochlear hair cells, and some are expressed just before or after maturation of mechanosensitivity. We found that many of the known hereditary deafness genes are much more highly expressed in hair cells than surrounding cells, suggesting that genes preferentially expressed in hair cells are good candidates for unknown deafness genes.

**Key words:** cochlea; development; FACS; hair cell; RNA-Seq; vestibule

## Introduction

Hair cells (HCs), the mechanoreceptor cells for hearing and balance, are epithelial cells that have undergone terminal division and differentiation. They are embedded in sensory epithelia adjacent to cells that do not have a mechanosensory function. Understanding the gene-expression patterns that differentiate HCs from various surrounding cells (SCs) can help elucidate the proteins that give HCs their unique function.

Because HCs do not divide they must last the life of an animal, which can be many decades in the case of humans. Death of HCs over time leads to deficits in hearing and balance (Groves, 2010). Much research on treatment for age-related hearing loss is focused on identifying the patterns of gene expression that lead to

an HC phenotype, so that induction of these genes in remaining supporting cells might restore function (for review, see Gélécoc and Holt, 2014). But first we need to understand gene expression during development.

Some hearing loss has hereditary causes. Congenital deafness occurs in 1 of approximately 500 births and >50% of cases are caused by gene defects (Smith et al., 1993). Many such genes are enriched in HCs: although HCs constitute only approximately one-tenth of the cells in the sensory epithelium of the cochlea, approximately one-third of the genes causing inner ear malformations or dysfunction in the mouse involve HC pathology (85 of 277; [http://hearingimpairment.jax.org/master\\_table1.html](http://hearingimpairment.jax.org/master_table1.html)). In humans, nearly 300 genetic loci for hearing impairment have been described, but the causative genes for ~100 have been identified (116; <http://hereditaryhearingloss.org>). Understanding the complete transcriptome of HCs may thus facilitate the discovery of new deafness genes.

We previously performed transcriptome studies of HCs by differential analysis between normal whole-sensory epithelia and mutant epithelia, either lacking HCs (*Atoh1*<sup>-/-</sup>; Scheffer et al., 2007a, b) or lacking hair bundles (*Pou4f3*<sup>-/-</sup>; Z.-Y. Chen and D.P. Corey, unpublished observations). But elimination or inactivation of one cell type can affect gene expression by remaining cells, compromising gene identification by differential comparison. It would be better to isolate pure populations of normal cells. Here, we used a mouse strain that expresses eGFP driven by the promoter for *Pou4f3* (Huang et al., 2013), an HC transcription factor. We developed an enzymatic treatment to dissociate cells of the sensory epithelia, and FACS to purify HC. With next-generation or high-throughput sequencing (HTS), we performed an unbiased and quantitative transcriptome study at four devel-

Received Dec. 17, 2014; revised Feb. 17, 2015; accepted March 6, 2015.

Author contributions: D.I.S., J.S., D.P.C., and Z.-Y.C. designed research; D.I.S. and J.S. performed research; D.I.S. and J.S. analyzed data; D.I.S., J.S., and D.P.C. wrote the paper.

This research was supported by National Institutes of Health grants R01-DC000304 and R01-DC002281 (D.P.C.), R03-DC013866 (J.S.), and R01-DC006908 (Z.-Y.C.); by the Frederick and Ines Yeatts Hair Cell Regeneration Grant (Z.-Y.C.); by P30 DC05209 to the Eaton-Peabody Laboratory of M.E.E.; and by a Hearing Health Foundation Emerging Research Grant (J.S.). D.P.C. is an Investigator and J.S. was an Associate of the Howard Hughes Medical Institute. We appreciate assistance from the Harvard Stem Cell Institute Flow Cytometry Core Facility at Massachusetts General Hospital and from the Harvard Medical School Biopolymer Facility. We also appreciate the gift of a DNASH probe from Anja Beckers at Hannover Medical School. We thank the Neurobiology Imaging Facility (a part of the Neural Imaging Center supported by National Institute of Neurological Disorders and Stroke P30 Core Center Grant NS072030) for consultation and instrumentation and Dr. Lisa Goodrich for useful comments on this manuscript.

\*D.I.S. and J.S. contributed equally to this work.

The authors declare no competing financial interests.

Correspondence should be addressed to either of the following: David P. Corey, Department of Neurobiology and Howard Hughes Medical Institute, Harvard Medical School, 220 Longwood Avenue, Boston, MA 02115, E-mail: dcorey@hms.harvard.edu; or Zheng-Yi Chen, Department of Otolaryngology and Laryngology, Harvard Medical School and Massachusetts Eye & Ear, Boston, MA 02114. E-mail: zheng-yi\_chen@meei.harvard.edu.

DOI:10.1523/JNEUROSCI.5126-14.2015

Copyright © 2015 the authors 0270-6474/15/356366-15\$15.00/0

opmental time points, before and during the acquisition of mechanosensitivity. We compared gene expression by HCs to that of the other cells in the sensory epithelium, collectively referred to as surrounding cells. Groups of genes differentially expressed in one or another cell type were linked to function. To make these data and comparative expression metrics publically available, we created the Shared Harvard Inner Ear Laboratory Database ([shield.hms.harvard.edu](http://shield.hms.harvard.edu)), which presents gene expression data integrated with comprehensive annotation including potential deafness loci.

## Materials and Methods

**Animal protocols.** All experiments were performed in compliance with ethical regulations and approved by the Animal Care Committees of Massachusetts Eye and Ear and Harvard Medical School.

**Cell dissociation, FACS, and RNA extraction.** We used a transgenic mouse strain expressing GFP under the control of the *Pou4f3* promoter (*Tg(Pou4f3-Is1-eGFP)*). These mice have normal morphology, normal expression of differentiation markers, and normal function until 17 months old (Huang et al., 2013). We also used a strain expressing *tdTomato* under the control of the *Gfi1* promoter (*Gfi1<sup>tm1(Cre)Gan</sup>, R26<sup>tdTomato</sup>*). In both strains, the only fluorescent cells in the inner ear are HCs. Animals from either sex were used. Utricles were dissected from the temporal bone and (at postnatal stages) incubated for 2 min in protease XXIV (0.1 mg/ml) to remove the otoconia. Cochleae were dissected and freed from the spiral ganglion and Reissner's membrane to expose the sensory epithelium. All dissections were done in ice-cold PBS, and utricles and cochleae were dissected in <1 h. The organs were collected in DMEM (Life Technologies) + 5% FBS on ice. The cells were dissociated by incubating the organs at 37°C in 1 mg/ml dispase (Gibco) and 1 mg/ml collagenase I (Worthington) in 100  $\mu$ l for ~10–12 utricles or 200  $\mu$ l for 10–12 cochleae for 30 min at E16 and P0 or 45 min at P4 and P7 and triturating with a pipette. The dissociation was controlled visually with an inverted microscope. Dissociation buffer (Gibco 13151–014 + 5% FBS) was added to complete the dissociation and the samples were placed on ice. The dissociated tissues were filtered through a 40  $\mu$ m cell strainer to eliminate clumps before sorting. Cells were sorted on a BD FACS Aria II cell sorter using a 100  $\mu$ m nozzle and low pressure. Hair cells were collected using the brightest GFP fluorescence signal and other cells were collected using the lowest fluorescence signal. The number of collected cells is indicated in Figure 1D. Cells were collected directly into a lysis buffer from the RNeasy Plus Micro kit (Qiagen). Total RNA extraction was performed using the manufacturer's recommendation and the quality was assessed with Agilent 2100 Bioanalyzer picoChips.

**Study design and statistics.** In this series of 16 samples, we used a matrix design of three factors: cell types (HCs and SCs), tissues sources (cochlea and utricle), and developmental stages (E16, P0, P4, and P7). We did not include a biological duplicate of the same condition; instead, for differential gene expression analysis of each factor, we combined samples of different levels in other factors and treated them as replicates to allow statistical analysis. This practice overestimated the variance due to other factors; therefore, the FDR values were more conservatively estimated than those calculated when true biological replicates were used.

**HTS.** mRNA was amplified using the Ovation 3'-DGE System (NuGEN). 3'-enriched transcriptome tags [~500 bp on average from the poly(A) tail] were converted into nondirectional Illumina sequencing libraries at the Biopolymer Facility at Harvard Medical School. Synthetic spike-in standards were not used, because the goal was not absolute quantification, but relative differential expression. Single-end reads of 35 bp or 50 bp were sequenced using standard protocols on an Illumina HiSeq Sequencer. Paired-end reads were used for GFP<sup>+</sup> cochlea and utricle at P0 and some sample libraries were rerun when the original read depths were not sufficient. The sequence quality was assessed using the open-source FastQC program. Quality-filtered reads were mapped against NCBI build 37/mm9 mouse genome assembly at DNAexus ([dnanexus.com](http://dnanexus.com)). Assignments of nonunique alignments were weighed by the posterior probability of their mapping. The read counts of 20,207 RefSeq mouse genes were calculated using the 3SEQ transcriptome-

based quantification analysis pipeline (<https://classic.dnanexus.com/whitepapers/DNAexus-whitepaper-rna-3seq-transcriptome.pdf>). Custom scripts were developed to generate raw read-count tables. These data were summarized, normalized, and statistically tested for differential gene expression for each gene under various comparison schemes using the DESeq package in R/Bioconductor (Anders and Huber, 2010). Multiple testing corrections were performed using the Benjamini and Hochberg methods and the false discovery rate (FDR) was calculated for each gene.

We chose nondirectional single-end sequencing of 3'-tagged mRNA. RNA-Seq of the 3' end more accurately quantifies transcripts than RNA-Seq of full-length transcripts, because length and GC content contribute most to sequencing bias (Asmann et al., 2009; Morrissey et al., 2009). Because recovered HCs were few in number, we had to amplify the transcripts to reach sufficient amount to construct the HTS libraries. Amplification inevitably introduces bias, which would be exacerbated by variable lengths of different genes if samples were random primed and the integrity of the RNA samples would be variably affected. Using RPKM/FPKM to represent gene expression values would not be as accurate because of variable actual length of transcripts amplified, especially for genes expressed at low levels and with complex genomic organization (Steijger et al., 2013). On the other hand, 3'-tags of the transcripts are of similar lengths, less susceptible to RNA degradation, and universally amplified from the polyA tail. Read counts are therefore less biased and they more faithfully reflect gene expression levels in the cells. Because the 3'-tags are short (with a mode of ~500 bp) and because we aimed to quantify the expression level, single-end sequencing was sufficient to generate the read counts. Because few genes have overlapping 3'-ends in opposite direction in mammalian genomes, we opted for nondirectional sequencing.

The dChip V2010.01 software (<https://sites.google.com/site/dchipsoft/>) was used to visualize the expression data by hierarchically clustering genes. The distance metric between two genes was calculated as correlation of the expression of the 3'-tags of two genes across samples, and the centroid linkage method was used to compute the distances between a gene and a gene cluster, and between two gene clusters (Golub et al., 1999). This involved log transformation of the normalized expression values from the DESeq analysis, computing the standardized expression values (scaled to have mean 0 and SD 1) of a gene across samples, averaging the standardized values of genes sample wise in a gene cluster, and using this averaged expression profile as the expression vector of a gene cluster to compute distance between gene clusters.

The raw data are available on the GEO database, accession number GSE60019.

**RT-PCR.** RNA was extracted from P6 cochleae, utricles, and hearts of CD1 mice using QIAzol (Qiagen), treated with DNase I (Roche), and reverse transcribed using random hexamer primer, with Superscript II (Invitrogen) to generate cDNA. PCRs were performed with recombinant TaqDNA polymerase (Invitrogen).

**Quantitative PCR.** Real-time analysis was performed using TaqMan gene expression assays (Life Technologies) on an Mx3000P QPCR system (Agilent Technologies). All reactions were run in duplicate using the Platinum Quantitative PCR SuperMix-UDG w/ROX (Life Technologies). Data were normalized to the housekeeping gene *Pgk1* and analyzed using the deltaCt method. Probes used include the following: *Mm01181529\_s1* (*Atoh1*), *Mm00438168\_m1* (*Cdkn1b/p27kip1*), *Mm00517585\_m1* (*Isl1*), *Mm01274015\_m1* (*Myo7a*), *Mm01168739\_m1* (*Pcdh15*), *Mm00436617\_m1* (*Pgk1*), *Mm00454761\_m1* (*Pou4f3*), *Mm00435971\_m1* (*Prox1*), and *Mm03053810\_s1* (*Sox2*) from Life Technologies. The *Cdh23* probe was designed to recognize isoforms E and F (accession EU681829 and EU681830): forward primer (5'-GTGATCA CACGGAAAGGTGAATA-3', Probe/56-FAM/CCACATTCC/ZEN/ACA ACCAGCCCTACA/3IABkFQ/), and reverse primer 5'-TTGACGATGAGATGGGTGTC-3', synthesized by Integrated DNA Technologies.

PCR primers include the following: *Gapdh*: Forward 5'-CTCATGAC-CACAGTCCATGC-3', Reverse 5'-AGGTCCACCACCTGTTGC-3'; *Emcn* ISH probe: Forward 5'-CAGATGGAACACCTCCCG-3', Reverse 5'-TCCACGGATCGAGGCTA-3'; *Ptgds* ISH probe: Forward 5'-GACA-CAGTGCAGCCCAAACITTCAA-3', Reverse 5'-TGACTGACTTCTCT-

CACCTGCGTT-3'; *Strip2* ISH probe: Forward 5'-GAATATGGAGA TTCAGACGGGC-3', Reverse 5'-AAACATGACCACCTTCCAGAGC-3'; and *Lmod3* ISH probe: Forward 5'-GTGAGGAGCTCGAT GAAGACG-3', Reverse 5'-TCGTCATCTTCCTCCTCCCTCC-3'.

**In situ hybridization.** Probes were obtained from Anja Beckers (*Dnah5*; Beckers et al., 2007), I.M.A.G.E clone (ID 4984025; *Grp*), or amplified from mouse cochlear cDNA (see primer list), and cloned into the pCRII-Topo vector (Invitrogen). Inner ears of CD1 mice were collected at stages E16 and P6, fixed in 4% formaldehyde, and cryosectioned (7- to 10- $\mu$ m-thick frozen sections). *In situ* hybridization was performed as previously described (Scheffer et al., 2007b).

**Immunocytochemistry.** For cryosections, inner ears of P6 CD1 mice of either sex were collected, fixed in 4% paraformaldehyde, and cryosectioned (7–10  $\mu$ m thick). A microwave antigen-retrieval technique was applied (H-3300; Vector Laboratories) before permeabilization and blocking in 1× PBS + 0.05% Triton + 8% normal goat serum for 1 h at room temperature. The sections were then incubated with primary antibodies overnight at 4°C and secondary antibodies for 1 h in blocking solution at room temperature. Stained slices and tissues were mount with ProLong Gold Antifade Reagent with DAPI (Invitrogen).

For whole mount inner ears of CD1 mice were fixed in 4% paraformaldehyde and dissected to expose the organs of Corti. Tissues were permeabilizedblocked in 1× PBS + 0.3% Triton + 8% normal goat serum (1 h, room temperature), then incubated with primary antibodies overnight (4°C) and secondary antibodies for 1 h in blocking solution (room temperature).

Primary antibodies were rabbit polyclonal anti-MYO7A (1/2000; Proteus Biosciences; 25-6790), mouse monoclonal anti-MYO7A (1/2000; Developmental Studies Hybridoma Bank, University of Iowa; 138-1), mouse monoclonal anti-LDB3 (1/300; Abnova; H00011155-M06), rabbit polyclonal anti-PMCA2 (1/200; Dumont et al., 2001), rabbit polyclonal anti-LMOD3 (1/1500; Proteintech; 14948-1-AP), and rabbit polyclonal anti-LMOD1 (1/1000; Proteintech; 15117-1-AP). Secondary antibodies were Alexa Fluor 488 or 594 goat anti-rabbit or anti-mouse antibodies (Invitrogen). Actin was counterstained with Alexa Fluor 594 phalloidin (Invitrogen).

**Biological process ontology analysis.** To ascertain the extent of functional enrichment we performed an analysis with the functional annotation tool DAVID 6.7 (Huang da et al., 2009a, b), which determines whether biological processes are enriched within a target list of genes. Genes were considered enriched in cochlear and utricular HCs when total read count was >50 and, at the considered age,  $(GFP^+ - GFP^-)/(GFP^+ + GFP^-) > 0.67$ .

**Principal component analysis.** Normalized gene expression values were assembled into a matrix with rows of different sample types and columns of genes. Genes with a total number of reads across all ages <10 were excluded and the numbers <1 at a single age were rounded to 1. The matrix was log2 transformed and the principal component analysis (PCA) was performed on the data using the statistics package in R. Each gene was considered a variable vector.

## Results

### RNA-Seq of purified mouse hair cells

To purify HCs, we used a transgenic mouse strain expressing GFP under the control of the *Pou4f3* promoter. In this strain, the GFP signal is specific for cochlear inner and outer hair cells (IHCs and OHCs) and for vestibular HCs (Fig. 1A; Keithley et al., 1999; Huang et al., 2013). SCs, which include supporting cells in the sensory epithelium and nearby cells of the inner ear epithelia, were not fluorescent. We dissected the sensory epithelia from the cochlea and utricle at four stages of development—E16, P0, P4, and P7—which correspond to ages before, during, and after acquisition of mechanosensitivity. The cochlear epithelium was trimmed to include the organ of Corti, the spiral limbus, and basilar membrane but not spiral ganglion or lateral wall, and the utricular epithelium was trimmed to the edge of the macula (Fig. 1B). Cells from cochleae and utricles expressing GFP (GFP $^+$ )

were separated from GFP $^-$  cells using enzymatic dissociation followed by FACS. The strong GFP signal in HCs and the size differential enabled specific separation of the HCs from SCs (Fig. 1C). Flow cytometry showed that the strongly GFP $^+$  HCs constituted  $1.2 \pm 0.2$  and  $0.30 \pm 0.08\%$  of all cells in the utricular and cochlear samples, respectively. The number of cells harvested for each sample is indicated in Figure 1D.

Transcriptomes of the purified HCs and SCs were then studied by HTS. To quantify coding RNAs accurately, polyadenylated mRNA was amplified and 3'-enriched transcriptome tags were converted into nondirectional cDNA sequencing libraries. Each of 16 samples (HCs and SCs from cochlea and utricle at four developmental stages) was sequenced to a depth of 40–100 million reads.

### PCA

Gene expression varied widely across the 16 samples. To understand the primary determinants of gene expression, we used PCA to identify the drivers of differences. The normalized GFP $^+$  and GFP $^-$  matrices were merged based on gene names; the merged matrix was then analyzed by PCA. The first three principal components explained >50% of the variance. A biplot of principal components 1 and 2 is shown in Figure 2A. HC samples are green and SC samples purple; samples from cochlea are in dark colors and utricle in light colors. The first component (PC1; accounting for 22% of the variance) is strongly associated with the cell type: all the SC samples (left) are separated from all the HC samples (right). The second component (PC2; accounting for 17% of the variance) is loosely related to the developmental stage, with the oldest stages (P4 and P7) represented at the top of the plot and P0 at the bottom. The third and subsequent components do not show obvious correlation with identifiable factors, suggesting high complexity of gene expression patterns in HC and other cells in the inner ear during development.

### Reproducibility of expression data

To study the widest range of cell types and developmental points, we did a single set of four RNA-Seq experiments at each age. To understand whether duplicates would produce the same results, we repeated the experiment at one age using a second mouse strain in which the fluorescent protein tdTomato is expressed under control of the *Gfi1* promoter (*Gfi1*<sup>tm1(Cre)Gan</sup>;R26<sup>tdTomato</sup>). We dissociated and sorted cells from P0 mice using FACS as before, but with settings appropriate for tdTomato fluorescence. The experiment was run in duplicate, with independent dissections, sorting, and RNA-Seq. RNA-Seq was highly reproducible. Technical replicates obtained by sequencing the same library multiple times showed over 95% correlation. RNA-Seq results of biological replicates in P0 *Gfi1*<sup>tm1(Cre)Gan</sup>;R26<sup>tdTomato</sup> HCs and SCs in cochlea and utricle at P0 were correlated by 84–93%. PCA confirmed the reproducibility among samples from the same cell type, age, and tissue source, even those from different transgenic mouse strains (Fig. 2A). Data from the P0 tdTomato experiments are represented in the PCA plot (Fig. 2A) as “-T,” with the duplicates denoted as -T1 and -T2. For each cell type, duplicates tend to cluster with each other in the PCA plot, and they cluster with the data from GFP-expressing mice. Although there is no perfect overlap, these experiments provide confidence that the patterns of gene expression during development are generally reproducible.

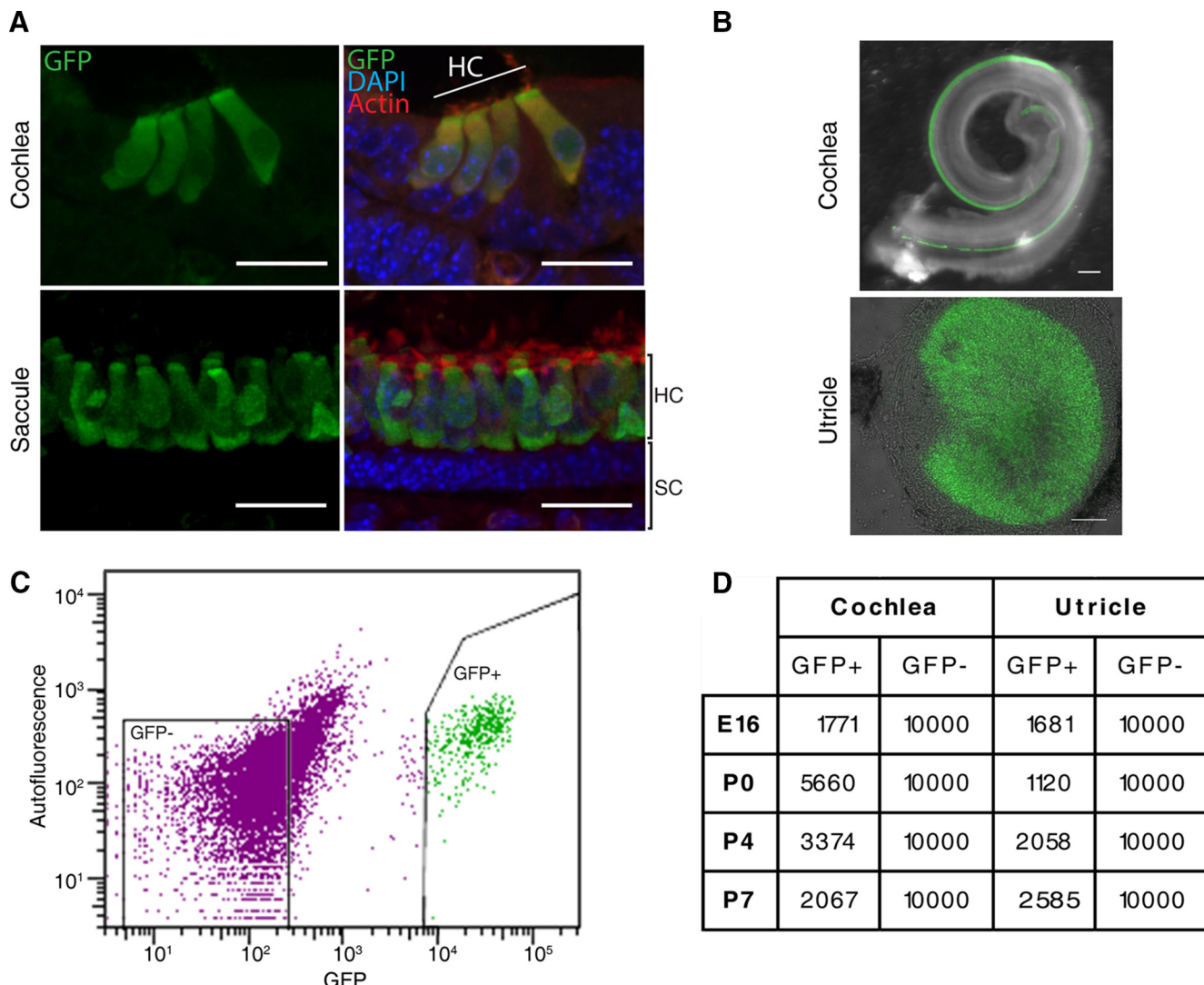


**Figure 1.** FACS purification and RNA-Seq results. **A**, GFP signal in transverse sections of cochlear and utricular HCs from P4 Tg(Pou4f3-*lsl*1-eGFP) mice. Note the specific GFP expression in cochlear IHCs and OHCs. Supporting cells and other SCs are not labeled. DAPI and fluorescent phalloidin counterstains outlined surrounding areas. **B**, Dissected tissues used for FACS at P4, shown as combined fluorescence and bright field. Hair cells expressing GFP are green. Cochlear samples included hair cells and supporting cells of the organ of Corti, spiral limbus, basilar membrane, part of the spiral ligament, and spiral ganglion neuronal processes. Utricle sensory epithelium was trimmed away from crista ampullaris, vestibular ganglion, and the roof of the utricle. **C**, FACS analysis of dissociated sensory epithelia. Gating on GFP<sup>+</sup> DAPI<sup>-</sup> cells, coupled to the size of the cells, allowed specific separation of the hair cells from surrounding cells and exclusion of dead cells and doublets. To avoid contamination, only cells exhibiting the highest intensity levels in the GFP channel were harvested as GFP<sup>+</sup> cells. GFP<sup>-</sup> cells were those with low GFP fluorescence, as delineated. **D**, Number of GFP<sup>+</sup> and GFP<sup>-</sup> cells harvested by FACS at all ages in cochlea and utricle.

#### Genes enriched in HCs

We examined the differential mRNA expression in HCs and SCs by pairwise comparison between the GFP<sup>+</sup> and GFP<sup>-</sup> samples using the normalized read counts at four ages. The number of reads reflect the abundance of mRNA in each sample. These were divided into three different categories of genes: the HC-enriched genes (green; GFP<sup>+</sup>/GFP<sup>-</sup> > 2), the SC-enriched genes (purple; GFP<sup>+</sup>/GFP<sup>-</sup> < 0.5), and the nonspecific genes (black; 0.5 < GFP<sup>+</sup>/GFP<sup>-</sup> < 2; Fig. 2B,C). Among the 20,207 annotated mouse genes, only 2008 genes were not expressed (<15 total read counts). Among the remaining 18,199 genes, 5430 were found to be preferentially expressed in HCs (including the genes with no reads in the SCs) and 3230 in SCs; 9539 were expressed in both.

#### Differences between cochlear and utricular HCs

To identify genes encoding proteins important for mature HC function, we divided them further by expression in cochlear HCs,

utricle HCs, or both (Fig. 2D). We selected 916 genes by choosing those enriched 4× with FDR < 0.05 in postnatal (P0, P4, and P7) cochlear HCs compared with postnatal cochlear SCs, or enriched in postnatal utricular HCs with the same criteria. Utricle HC reads were plotted against cochlear HC reads for each gene. Genes were marked as cochlea-enriched if cochlear reads were >5× utricle reads (222 genes; dark green), or as utricle enriched (41 genes; light green), or as expressed in both (653; black). Selected genes are labeled with gene names. As the cochlea sample is dominated by OHCs, some of these genes may be involved in functions unique to OHCs, such as the generation and regulation of electromotility. Indeed, one of the most differentially expressed genes is *Slc26a5*, encoding prestin. Genes highly enriched in postnatal utricular cells include those encoding axonemal dyneins (*Dnah5*, *Dnah9*, *Dnah10*, and *Dnah11*), a flagellar protein (*Tekt2*), and a centrosomal protein (*Ccdc81*)—consistent with the presence of kinocilia in mature utricular but not cochlear HCs.

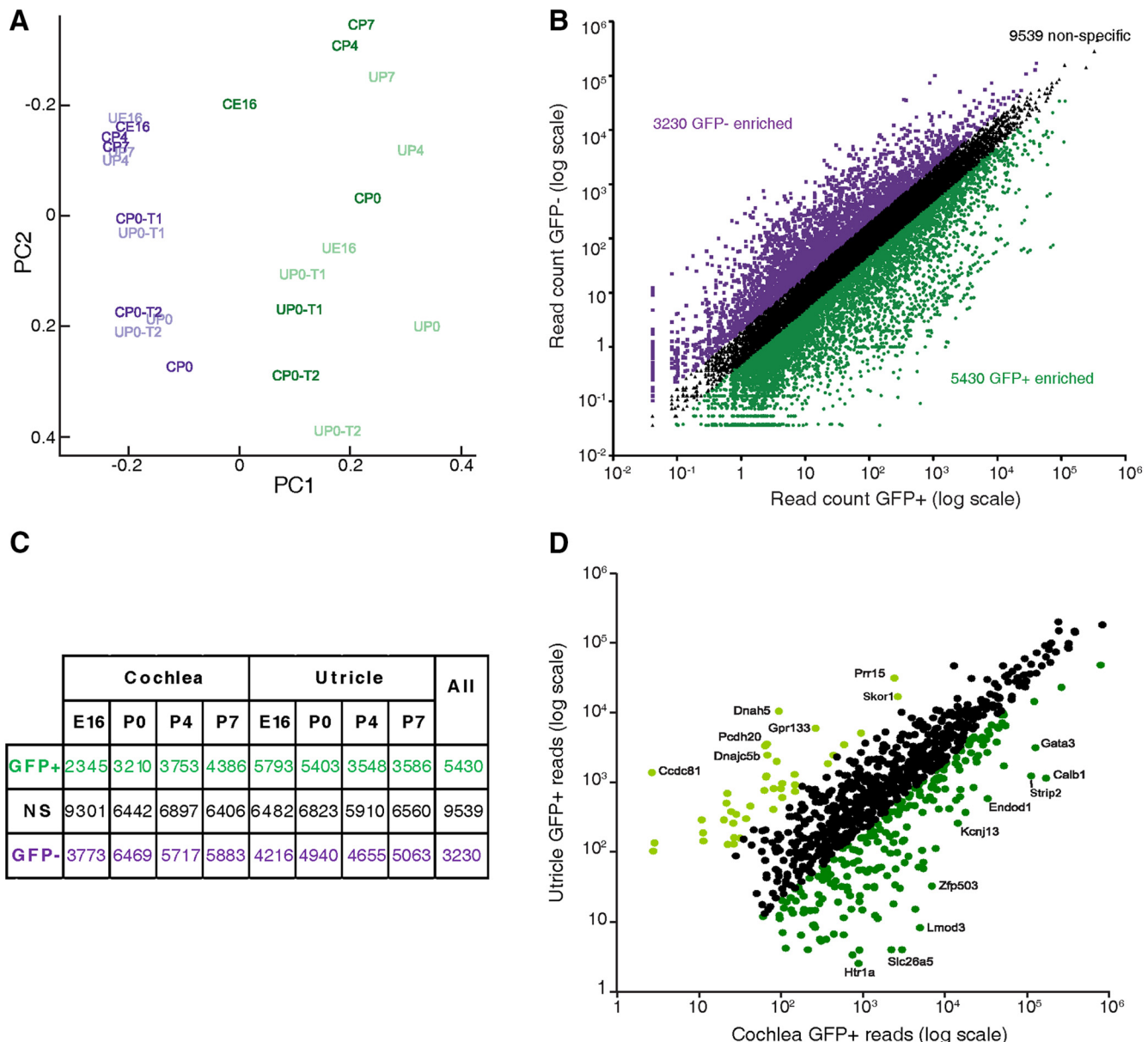


**Figure 2.** Tissue and age differences in expression. **A**, Principal component analysis plot of all 16 samples (light colors for utricle and dark for cochlea) for all 20,207 genes represented in the NCBI build 37/mm9 mouse genome assembly. PC1 correlated with cell type: GFP<sup>-</sup> (purple) to the left and GFP<sup>+</sup> (green) to the right, and PC2 correlated approximately with age. Most points are expression from *Pou4f3-eGFP* mice; those denoted as -T1 and -T2 are from mice expressing tdTomato under control of *Gfi1*. **B**, **C**, Analysis of the HTS results. Differential expression in GFP<sup>+</sup> and GFP<sup>-</sup> samples was assessed using the average number of reads at all four ages. Only genes with a minimum of 15 total reads across all samples were considered. There were 5364 enriched in hair cells (GFP<sup>+</sup>/GFP<sup>-</sup> > 2), 3230 genes were enriched in surrounding cells (GFP<sup>+</sup>/GFP<sup>-</sup> < 0.5), and 9539 genes were nonspecific (0.5 < GFP<sup>+</sup>/GFP<sup>-</sup> < 2). **D**, Differential mRNA expression in postnatal utricular and cochlear HC samples. Genes included in this plot were at least four-fold enriched in HCs compared with SCs in either utricle or cochlea (or both). HC genes preferentially expressed (>5×) are shown in light green (utricle) or dark green (cochlea); not preferentially expressed are black.

### Gene-expression analysis

To determine the specificity of the HTS results, we examined the expression patterns of genes previously known to be enriched in HCs relative to SCs. Figure 3 shows, for selected genes, the number of reads in utricular and cochlear HCs compared with SCs at each age. Transcripts from well known HC genes such as *Atoh1*, *Gfi1*, *Slc26a5*, *Tmc1*, *Lhfp15*, *Pcdh15*, *Fscn2*, and *Chrna9* were found, as expected, to be highly enriched in HCs (green bars) compared with SCs (purple bars; Zuo, 2002; Peng et al., 2011; Schimmang, 2013). The enrichment of each gene in HCs, averaged across organs and ages, is indicated by the fold-change (FC) value (FC = GFP<sup>+</sup>/GFP<sup>-</sup>), which ranged from 35 (*Pcdh15*) to 1395 (*Gfi1*), and by the FDR (Fig. 3). Similarly, genes known to be en-

riched in SCs, such as *Wnt5a* and the deafness gene *Coch* (Robertson et al., 2001; Qian et al., 2007), have few reads in GFP<sup>+</sup> cells (Fig. 3). Fold-change values for these two are 0.06 and 0.008, respectively.

These data, from developmental ages E16 to P7, reveal the time course of gene expression in addition to enrichment in different cell types. For instance the transcription factor *Atoh1*, involved in the differentiation of HCs as early as E12.5, is known to be downregulated at postnatal stages when HCs mature (Birmingham et al., 1999; Scheffer et al., 2007a). As expected, HTS data show expression of *Atoh1* decreasing between E16 and P7 in the utricle and between P0 and P7 in the cochlea—consistent with the earlier maturation of the utricle compared with the cochlea (Fig. 3).

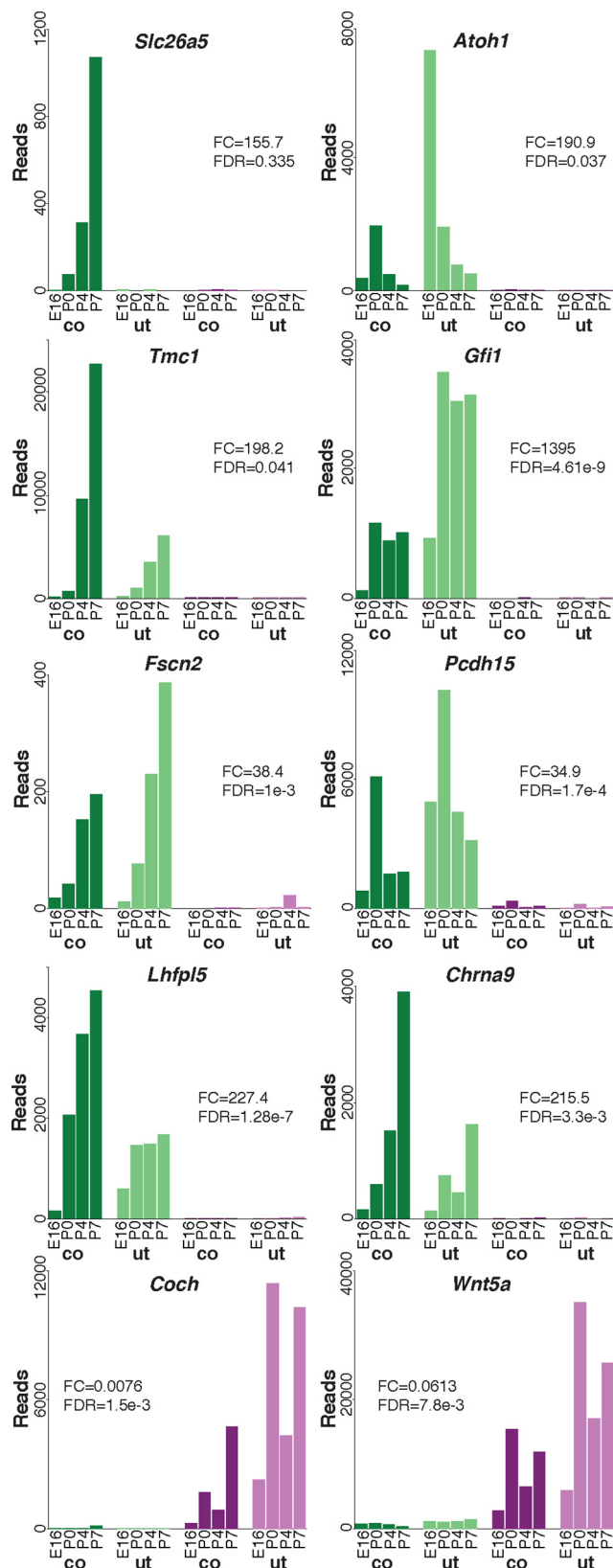


**Figure 3.** Representative HTS expression profiles for *Slc26a5* (prestin), *Atoh1*, *Tmc1*, *Gfi1*, *Fscn2*, *Pcdh15*, *Lhfp15*, *Chrna9*, *Coch*, and *Wnt5a*. Histograms display the normalized number of reads in hair cells (green) and surrounding cells (purple) in samples from the cochlea (co; dark colors) and utricle (ut; light colors) at ages E16, P0, P4, and P7. Indicated for each gene are the FC representing the GFP<sup>+</sup>/GFP<sup>-</sup> counts ratio and the multiple test adjusted FDR determined by the Benjamini–Hochberg procedure.

## Purity of the FACS HCs

We examined differential expression in GFP<sup>+</sup> and GFP<sup>-</sup> cells of genes known to be expressed in HCs and supporting cells. In particular, we looked at the *Notch*, *Hes*, *Jag*, and *Delta* genes, which are Notch pathway effectors that determine the mosaic pattern of the inner ear sensory epithelia. As expected, *Jag2* and all the *Delta-like* (*Dll*) members were highly enriched in GFP<sup>+</sup> cells (Fig. 4A). *Notch1*, *Notch2*, *Notch3*, and *Hes1* were enriched in GFP<sup>-</sup> cells. *Jag1* and *Hes5*, previously shown to be expressed in both HCs and SCs (Zine et al., 2000; Hartman et al., 2009), had a broad expression pattern in our HTS data. Thus the dissociation protocol apparently separated HCs from SCs.

We also used gene expression to assess the purity of the samples. HCs and supporting cells are connected by both tight junctions and adherens junctions, so they can be difficult to separate. Despite the mesh filtering before FACS and the use of a size criterion to avoid doublets of cells during the sort, there might be a supporting cell contamination among the purified hair cells. At P7, when adherens junctions were mature and contamination might be highest, we identified nine genes that had at least 60 total reads in the two GFP<sup>+</sup> samples and had between 100- and 270-fold more reads in the GFP<sup>-</sup> samples. These include *Ptgds*, which encodes prostaglandin D2 synthase; *Col1a2*, which encodes collagen type 1a2; *Dcn*, which encodes the collagen-associated protein DECORIN; and *Coch*, which encodes the surrounding cell protein COCHLIN (others were *Atp1a2*, *Car3*, *Lef1*, *Apod*, and *Apoe*). If there was significant contamination from SCs, SC genes would have been detected at higher levels in the GFP<sup>+</sup> samples. Suppose, for instance, that a gene is expressed exclusively in SCs and that there are 8000 reads for that gene in the GFP<sup>-</sup> sample. If there is 1% contamination of SCs in the GFP<sup>+</sup> sample, we would expect 100-fold fewer reads in the GFP<sup>+</sup> sample, or 80 reads. Because we found at least nine genes with >100-fold fewer reads in GFP<sup>+</sup> than GFP<sup>-</sup> samples, we can conclude that the HC sample is at least 99% pure ( $1 - 1/100$ ).

A similar analysis found 14 genes (*Ocm*, *Smpx*, *Espnl*, *Tmc1*, *Srrm4*, *Calb1*, *Strip2*, *Kcnmb2*, *Pcp4*, *Pvalb*, *Nrxn3*, *Mreg*, *Apba1*, and *Bdnf*) that had 100- to 1000-fold more reads in the GFP<sup>+</sup> than GFP<sup>-</sup> samples at P7, indicating that the SC sample is also at least 99% pure.

## Validation of RNA-Seq results by quantitative PCR

To validate the differences in expression among cell types and developmental stages revealed by HTS, we used quantitative PCR (qPCR) to examine the expression of selected HC genes (*Pcdh15*, *Pou4f3*, *Cdh23*, *Atoh1*, and *Myo7A*). In HTS profiles from the cochlear samples from E16 to P7, these genes were found to have a significantly different expression pattern (Fig. 4B). qPCR on the same samples also showed differential expression and good agreement with HTS data. Similarly, we studied the expression of genes expressed in the prosensory domain during early development that later becomes supporting cell specific, such as *Prox1*, *Cdkn1b*, *Isl1*, and *Sox2* (Chen and Segil, 1999; Birmingham-McDonogh et al., 2006; Hume et al., 2007; Huang et al., 2008). Both HTS and qPCR showed a relative decrease in expression in GFP<sup>+</sup> cells from embryonic to postnatal cochleae, as expected (Fig. 4B).

## Deafness genes

Mutations of genes that are uniquely expressed in HCs are likely to cause deafness. We ranked, by enrichment level in HCs, the 18,199 genes expressed in our samples (Fig. 5A). We then identified the 112 known syndromic and nonsyndromic deafness genes

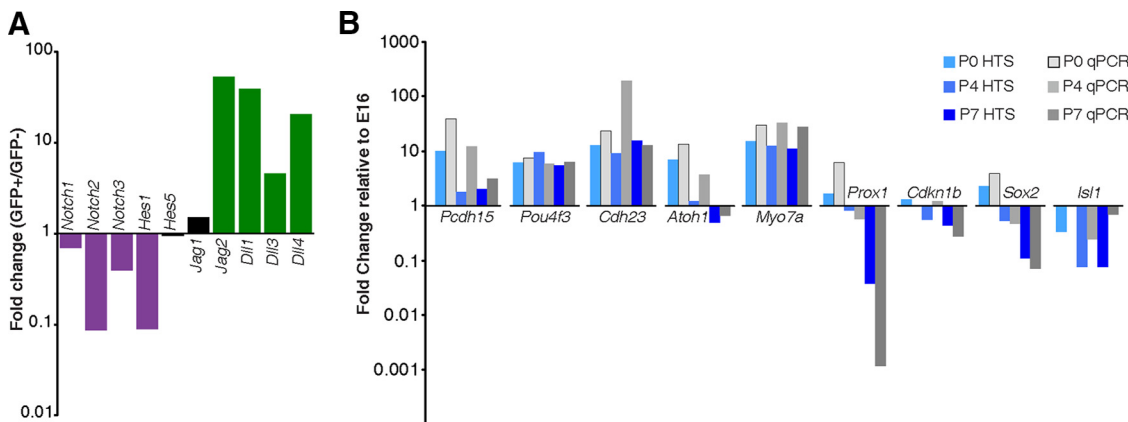


**Figure 4.** Validation of the HTS results. **A**, HTS expression profiles at all ages of key proteins of the Notch pathway. The Notch receptor genes, *Notch1*, *2*, and *3*, as well as the downstream effector, *Hes1*, were mostly expressed in surrounding cells (purple). *Hes5* and *Jag1* had nonspecific expression (black). The ligand-encoding genes *Jag2*, *Dll1*, *Dll3*, and *Dll4*, were enriched in hair cells (green). **B**, HTS results (blue) compared with qPCR (gray). The average counts and qPCR results in P0, P4, and P7 cochlea samples relative to the E16 sample were plotted as fold change.

(<http://hereditaryhearingloss.org>) and examined the positions of these genes within the ranked list. The deafness genes represented ~0.6% of the detected genes (109/18,199). We found that 50 of the deafness genes known to be HC specific, such as the Usher syndrome genes and myosin genes *Myo6* and *Myo7a*, were enriched in HCs according to HTS data. More than half of them (27) were included in the top 1000 genes of this ranking (Fig. 5A, B, first bin). With additional selection criteria, deafness gene candidates can be enriched further. For instance, if a search is restricted to those genes upregulated by  $>5\times$  during development and sorted by the  $\text{GFP}^+/\text{GFP}^-$  ratio, then 20 deafness genes are in the top 500, and 10 are in just the top 100. Genes differentially expressed in HCs are therefore a rich pool of deafness-gene candidates.

Similarly, more than half of the deafness genes enriched  $>2\times$  in SCs, such as *Coch* and *Pou3f4*, were in the 1000 genes most enriched in SCs (Fig. 5A, B, last two bins). Genes most enriched in HCs or SCs are more likely to encode proteins with specialized roles in the inner ear and, perhaps, are more likely to produce only hearing and balance disorders if mutated, so are good candidates for deafness genes.

#### Discovery of new HC and SC genes

To provide insight into gene networks involved in HC development and function, we grouped genes with similar patterns of expression. Such grouping has the potential to identify narrower classes of genes than a simple enrichment as in Figure 3. We constructed relative mRNA expression profiles and used dChip to arrange the genes according to their expression pattern. The hierarchical clustering heat maps showed subsets of genes enriched in SCs, in all HCs, in cochlear HCs, or in utricular HCs (Fig. 6, Tables 1 and 2). A variety of expression patterns was observed and these match expression patterns of constituent genes when known (Zine et al., 2000; Zuo, 2002; Jones et al., 2006; Hertzano et al., 2007; Scheffer et al., 2007b; Cotanche and Kaiser, 2010; M.J. Shin et al., 2010; Peng et al., 2011; Yoon et al., 2011; Carlisle et al., 2012; Schimmang, 2013; Hereditary Hearing Loss Homepage, <http://hereditaryhearingloss.org>). For instance, some genes were much more highly expressed in HCs than SCs, and were expressed at the earliest ages tested (Fig. 6A). Among them are *Atoh1*, *Gfi1*, *Pou4f3*, and *Lhx3*—all transcription factors essential for HC development.

HCs become mechanically sensitive between E16 and P0 in the utricle and between P0 and P4 in the cochlea (Géléoc and

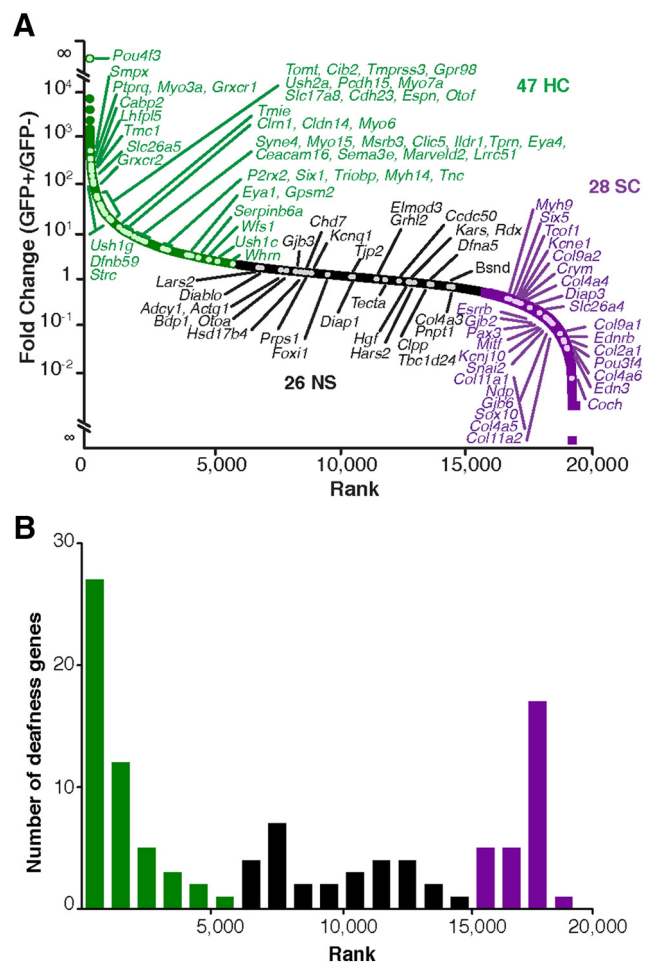


**Figure 5.** Deafness gene distribution. **A**, Expressed genes (total reads  $> 15$ ) ranked in order of the  $\text{GFP}^+/\text{GFP}^-$  read ratio at all ages. Green indicates the HC-enriched genes (fold change  $> 2$ ), purple the genes enriched in SCs (fold change  $< 0.5$ ), and black the nonspecific genes (NS). Known deafness genes are indicated in each category. **B**, Histogram showing the distribution of deafness genes relative to their  $\text{GFP}^+/\text{GFP}^-$  rank at all ages. Each bin represents 1000 genes. The majority of deafness genes previously shown to be expressed in hair cells was found in the top 2000 genes, and deafness genes expressed in surrounding cells were found within the last 3000 genes.

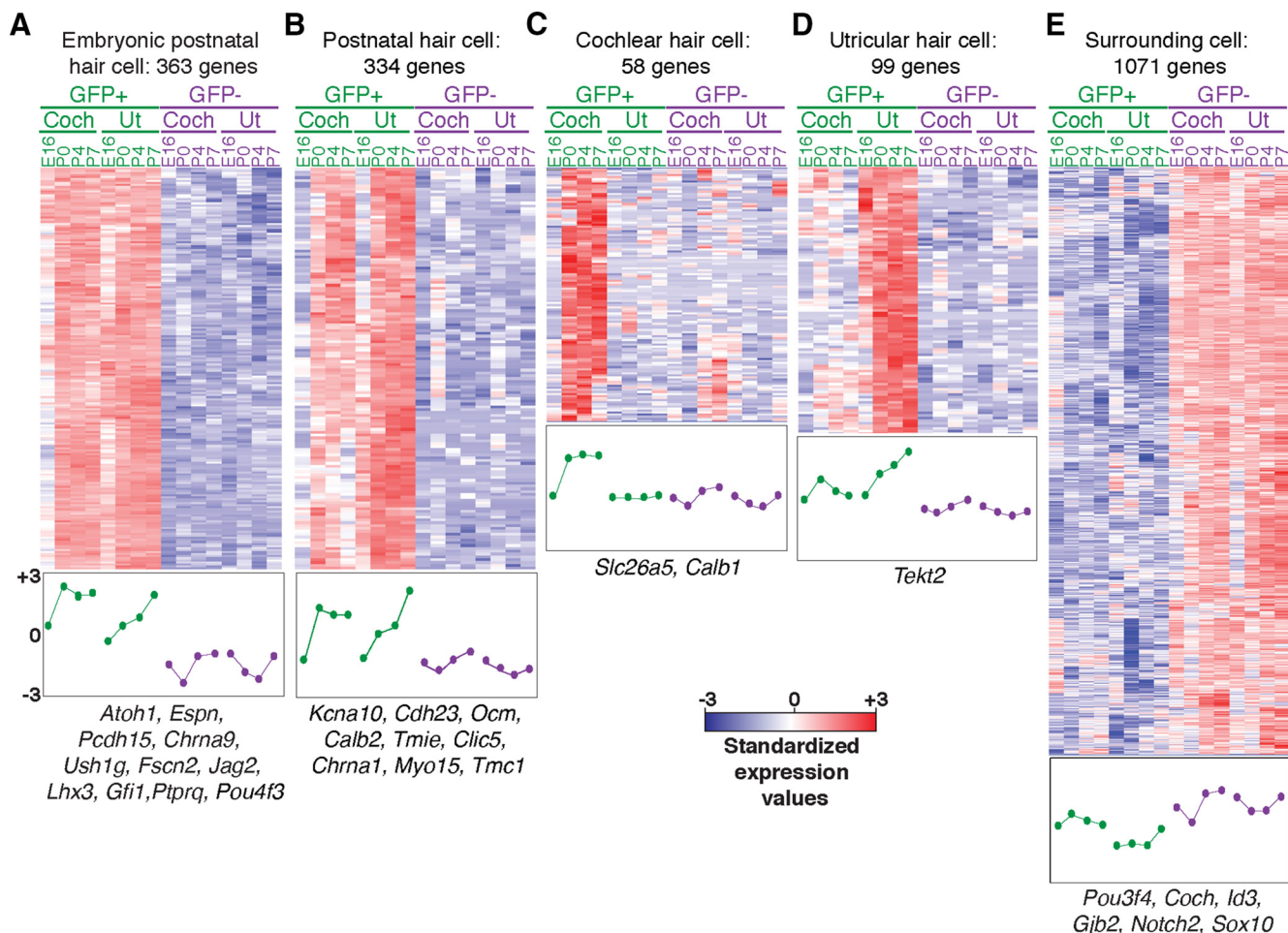


**Figure 6.** Spatial and temporal expression patterns of genes by hierarchical clustering. Heat maps are shown for selected tree branches clustered by spatial and temporal expression patterns; red represents above-average expression levels and blue below-average levels. Each row represents a gene, and each column a sample. Plotted below each heat map are the average standardized gene expression values across samples for that cluster. Examples of genes in the cluster are listed. The GFP<sup>+</sup> samples are shown in green and the GFP<sup>-</sup> samples in purple. Clusters represent embryonic and postnatal hair cell-enriched genes (**A**), postnatal hair cell-enriched genes (**B**), cochlear hair cell-enriched genes (**C**), utricular hair cell-enriched genes (**D**), and surrounding cell-enriched genes (**E**). See also Tables 1 and 2. Coch, cochlea; Ut, utricle.

Holt, 2003; Lelli et al., 2009). It is reasonable to suppose that genes critical for mechanotransduction are expressed in HCs but not SCs and are first expressed during those periods. Thus it was not surprising to find such genes enriched in HCs but not expressed early in the development of the cochlea (Fig. 6B). These include *Cdh23*, *Tmc1*, *Myo15*, and *Kcna10*, which are associated with mature HC function (Kawashima et al., 2011; Peng et al., 2011; Lee et al., 2013). Still others (Fig. 6C) were expressed only later in development, but only in cochlear HCs. Genes in this cluster may be associated especially with OHCs, as OHCs outnumber IHCs by three to one in the cochlear HC sample. Notable among these is *Slc26a5*, encoding the OHC motor prestin. A fourth cluster (Fig. 6D) is primarily expressed in utricular HCs. Some of these genes, such as *Dnah5*, *Dnah10*, *Dnah11*, and *Tekt2* (Yoon et al., 2011), encode known components of microtubule-based cilia, and their presence in this group may reflect the retention of kinocilia in the utricle and their degradation in cochlea. Another cluster (Fig. 6E) is expressed at much higher levels in SCs than in HCs. These include genes known to function in SCs, such as *Coch*, *Gjb2*, and *Notch2*. Table 1 lists the genes in each of the HC clusters and Table 2 lists the genes in the SC cluster. The clusters shown are just a subset of all branches in a hierarchical tree, but they illustrate the potential to identify genes that may have similar functions in HCs at similar stages of development.

#### Validation with *in situ* hybridization and immunocytochemistry

To validate the tissue and cell specificity revealed by the normalized read counts and the hierarchical clustering, we performed *in situ* hybridization and immunocytochemistry for selected genes (FC > 90; FDR < 0.1). Based on HTS reads, gastrin releasing peptide (*Grp*) and glutaredoxin cysteine rich 2 (*Grxcr2*) were expressed in both cochlear and vestibular HCs (Fig. 7A, B). Indeed, *in situ* hybridization in the organ of Corti and vestibular epithelium showed high levels of message in the HCs. Striatin interacting protein 2 (*Strip2*) and leiomodin 3 (*Lmod3*) were predicted to be expressed only by cochlear HCs (Fig. 7C, D). With *in situ* hybridization we found message only in the OHCs of the cochlea and not in vestibular epithelia. Dynein axonemal heavy chain 5 (*Dnah5*) was predicted to be highly expressed in vestibular but not cochlear HCs and this was confirmed by *in situ* hybridization (Fig. 7E). Endomucin (*Emcn*) was predicted to be in SCs, especially of the cochlea. With *in situ* hybridization we found high levels in cells of the basilar membrane (Fig. 7F), which were part of the SC samples. Finally, *Ptgds*, encoding a prostaglandin D2 synthase, was predicted to be mainly in vestibular SCs. We found expression in the dark cells of the ampulla (Fig. 7G), which are involved in pumping K<sup>+</sup> into endolymph. We also found *Ptgds* expressed in the stria vascularis of the cochlea, which is

**Table 1.** Genes expressed by embryonic and postnatal hair cells, postnatal hair cells, cochlear hair cells, and utricular hair cells as shown in Fig. 6

Embryonic and postnatal hair cells					Postnatal hair cells					Cochlear hair cells		Utricular hair cells	
Brun06	Em1	Capsl	Fam70b	Clec18a	Frmd4b	Ifit1	Slc25a33	Fsip1	Unc80	Slc16a5	Sgip1	Irx2	Gas2l2
Fam167a	Cyb561	Fam154b	Gf1 <sup>a</sup>	Slc18a1	Twf2	Lcn14	1190002A17Rik	Pts1	4932417116Rik	Tspyl5	Sycp2	Tctex1d1	Tekt4
Wdr31	Tspan13	A330021E22Rik	Lhx3 <sup>a</sup>	Dyx1c1	Tpbpb	Cyp17a1	C2cd2l	Ntfkbib	Nos1ap	Ccdc40	Calca	4732456N10Rik	Ddo
Eya4	Gabrb3	Fam183b	Acsf4	Kcn3	Dytn	Tas1r1	C130038G02Rik	Fam148c	Lrrc67	Rpgrip11	Dusp27	Foxj1	Gal
Impdh1	Gpr98 <sup>a</sup>	1700007K13Rik	Cdk4	Pih1d2	Myot	Tmem213	Morn2	Tmem173	Myo15 <sup>a</sup>	Rspn4a	Adck1	1810041L15Rik	1700026L06Rik
Dach2	Cib2 <sup>a</sup>	Armc4	B230396012Rik	Ribc2	Dock9	Slk32c	Zfr2	4930429B21Rik	Adcy8	Ip6k3	Grt1	Abcd2	Cyp1a2
Rassf10	St8sia3	Lrrc46	Ttc24	B4galT5	BC048546	A530016L24Rik	Selm	Pip4k2a	D10Bwg1379e	Zccch18	Icos	D11Bwg0517e	Ptpn22
Mpp7	Ttc21a	Wdr78	Cas21	Gm5567	Zmynd12	Sema6b	Jakmip1	Ttc30b	Lbxcor1	Cdh7	Wt1	6330439K17Rik	
Frmd5	Snapt91	Mtap9	Gm906	C230081A13Rik	Nod2	Bend6	Tuba4a	Ablim2	Txndc6	Tspan2	Slc34a3	Cdc151	Kif6
Pkp2	Parp6	Kcnh7	Chgb	Kifap3	Dbndd1	Tll3	Immp2l	Mtap7	Ryr2	4930528F23Rik	Ucp3	Dscam	Slc17a8
Fez1	Tspsyl4	Ccd68	Lmod1 <sup>b</sup>	Pgm2l1	Hist3h2ba	Amph	Tnfafp8l1	Spock1	Wdr16	1110004E09Rik	Klr1	Tmem130	4430420I18Rik
Me2	Wwc1	Wdr63	Rab11fip1	Wdr19	Nupl2	Accn3	Fzd6	Acpp	Agbl4	Awat2	Slc39a12	1700028P14Rik	Id4
Slc6a17	Prepl	Tcp11	Mfsd6	Sp110	Ppp13f	Nat14	Tceal5	Efn1	Dnajb13	Slc5a12	Acad11	Cdc113	Irak2
Ankrd24	Raver2	Chmn9 <sup>a</sup>	Plice1	Phf1	Rab12a	Slxbp1	1700030J22Rik	5730410E15Rik	Dystf1	Rph3a	Pkh111	Fbxo32	Ces2
Fam148b	Txnr1	Cldn9	Myob <sup>a</sup>	Gm88	Hrasl1	0610010012Rik	Uhmk1	Clic5	6430537H07Rik	Ugp2	Defb5	Brip1	Gm595
Cabp4	Ctrnd2	Dtna	Smpx	Serf1	Slc4a8	Hagh	Dyrk3	Rnf128	Tekt1	Sgs1m	Fabp12	Dnahc5 <sup>b</sup>	Lrrc27
Fam92b	Tmtc4	A730017C20Rik	Acss2	Ankrd42	Lmo3	Mmp24	Rem2	Cdc30	Cxcl14	Lrtm2	Ghsr	Cdc147	Ulk4
Dner	Myo16	Enkur	Atp6v1a	Tctn2	Rab36	Chchd10	Cistr3	Mycbp	Lrguk	Ubxn11	Gpr55	Rab3c	Car8
Cetn4	Epb4.115	Tmem30b	Ankrd22	Ttl7	Nrip3	Ctsf	Fbxo27	Osbpl3	4933413G19Rik	Fcho1	Slc9a2	Rxfp2	4932443J19Rik
493058N13Rik	Syt14	Ush1g <sup>a</sup>	Dusp14	Dmxl2	Ubxn10	Mps6	1810019J16Rik	Rtdr1	Nhlrc2	Tmc1 <sup>a</sup>	Fhit	Tekt2	Slc15a5
Morn5	2310030G06Rik	Spag6	Lrp11	Thns1	Igsf21	Rspf9	Mtrm7	Vwa3a	Oto <sup>a</sup>	Pcp4	Kndc1	Nxf3	Styx1
Fbxo16	R3hdml	Zfp474	Gm1322	Thsd7b	Megf11	Morn1	1700040J03Rik	Relt	170003M02Rik	Arv1	Fam160a1	1700019L03Rik	Gm14461
Spin1	Spn17	Atp11a	Xirp2 <sup>a</sup>	Dgkg	Syp	2210020M01Rik	Crb3	Wee2	Scn3b	Str <sup>a</sup>	Gcnt2	Fhad1	Mdh1b
Ssx2ip	Ppp1r3d	4930430F08Rik	Cpeb3	4930426L09Rik	Erc2	Efhc1	Nphp4	Kanat10 <sup>a</sup>	Chrn2	Mtmm11	Htr1a	Gm114	Csmd1
Fmn1	Rimklb	Ercc6	Gramd1c	Gm70	Pcdha2	Rspf1	Gnmt	Bcl2l14	Ccdc65	Trim45	Slc39a2	Plac1l	Trim9
Atp8b1	2900062L11Rik	Pacrg	Kcnab2	Artn	Ldhc	Fry	Gpr120	Tbc1d7	Ccdc96	Cd164l2	Adamts13	4930506M07Rik	Popdc3
2310030N02Rik	Herc3	Ap3m2	Nek11	Tmem184a	C77080	Nmnat3	Nipal3	Serpina3g	Fbxo36	Cyp4f39	Xkr9	Hopx	4732415M23Rik
Milt4	Ical1	Dynlrb2	Tom <sup>a</sup>	Mobkl2b	Ppm1e	Vepl1	Tjap1	1700061J05Rik	Sh3gl2	Arf3	D630029K05Rik	Perp	Lrrc51
Pawr	lldr1	Dctn3	Fam65b	Plch2	Cpne9	Gsg1	Ankfn1	Meig1	Pkig	Gm4371	Dera	Arid3c	
Rnf182	Rdh12	Hspa4l	3110043021Rik	Fam19a3	Htatip2	Tmem216	Pou4f2	Lrrc43	Gm9047	Cyp2j12	Nlx3–1	Casc1	
Ptpn2	Akap9	Myo3b	Gdpd1	Pgam2	Fbxo2	Fbxo15	Cacna2d4	4930434E21Rik	Hsd17b7	S100g	LOC100042450	Dyd2	
Zdhhc13	4932425124Rik	Mgst3	Mcf2l	Unc79	Cgn	Lbx2	Dnaja4	4930579J09Rik	Rab3ip	Syt6	Ptchd3	Liph	
Hook1	Ldb3 <sup>b</sup>	Ptpqr <sup>d</sup>	Tmem183a	Pvr1	Rab15	Clip4	Eno2	170003E16Rik	Aftph	Mycbpap	Dnahc11		
Lrp8	Arf6	Msrb3	Galnt9	Sgpp2	Rab3a	Kif27	Cds1	E230025N22Rik	Hsd17b14	Calb1 <sup>a</sup>	Crtac1		
Sall3	Prph2	Chst4	Gm757	Crtam	Cln6	Rab3b	Cyb561d2	1700024G13Rik	Cdk5rap2	Fam40b <sup>b</sup>	1700013F07Rik		
Syt7	Cyfip2	Cyld	Ccd103	Grp	Ormdl3	Cacna1d	Trpm2	Cdc87	5730508B09Rik	Sema5b	Kcn2e		
Vwa5b2	Lmo17	Gm5111	Fscr2 <sup>a</sup>	Rff1	Star10	Tom112	1110032A03Rik	Cybs5	4930558C23Rik	Rassf4	Tnr		
Espn <sup>a</sup>	Strbp	Myo3a <sup>a</sup>	Calm2	Acsf6	Gad2	Krt222	Armc3	2610034M16Rik	Efcab6	Nehf1	Tesc	1810046K07Rik	
Mtag2	Trit1	Faim2	Rnf157	Mfnf	Wbp1	Pck1	Gstm7	E230019M04Rik	2510049J12Rik	Umod1	Zbbx	Gm101	
Cln1	4921525H12Rik	Pitpna	1700009P17Rik	Btbd9	Rhpn1	Aacs	Tmem1	E230019M04Rik	2510049J12Rik	Umod1			
Sult4a1	Evl	Calm14	Kif9	Acot7	Aig1	1700017N19Rik	Cnnm2	Tekt3	Epn3	Scn1b	Ak7		
Myt1	Rims2	Chrn10	Lhfp14 <sup>a</sup>	Chchd6	2310047B19Rik	Chia	Adprh11	Ankrd5	Elov4	1190003J15Rik	Slc17a2		
Nhlh1	Nefm	Calm1	Otud3	Gpr4	Usp20	Dpf3	Fcrlb	Ccdc11	Cdh15	Lmod3 <sup>b</sup>	Ccdc19		
Hpcal1	Slca8a1	Pou4f3 <sup>a</sup>	Atad4	Neurla	Hist3h2a	Fgf21	Kcnj4 <sup>a</sup>	Dnal11	Cdk1l	Slc26a5 <sup>a</sup>	Zccch12		
Tcerg1l	Nrxn3	Camk2b	Rad15	2210411K11Rik	Zfp385a	Nppa	Calb2 <sup>a</sup>	Gca	Ttc39b	Zfp750	Krt20		
Cbln1	Pcdh15 <sup>a</sup>	Tmhs <sup>a</sup>	Eps8l2	Nup210	Pad2	Shank2	Chrn1 <sup>a</sup>	Gm11992	Wdr7	Rimb2	Gbx2		
Kcnmb2	5330437J02Rik	Gpr152	Gpr156	H33t6	St3gal5	Ccdc60	Apbb3	6030429G01Rik	S100a1	Actr3b	Lct		
Lmo1	Ube2u	Ap3b2	Lrrc48	Ubash3b	Gm166	Fhod3	Fabp1	Ccdc108	Slc7a4	Baiap2l2	Zp3		
Tmem41a	Barhl1 <sup>a</sup>	Espn <sup>a</sup>	Fam78b	Pcty1b	Ptpla	Ksr2	Abcc8	Dnah9	Tmprss3	Gpr151	Gck		
Stmn3	DIK2	Abcd7	Grcr1 <sup>a</sup>	Prkcz	Coq4	Lipm	Lrba	Dnajc5b	Sh2d7	Parp1	Stox1		
Disp2	Ush2a <sup>a</sup>	Apba1	Anxa4	Uck1	Ica1	Btn2a2	4930579G22Rik	1700012P22Rik	Myo7a <sup>a</sup>	Gst13	170002D08Rik		
Ckmt1	Nrsn1	Fank1	Mogat1	Brsk2	Nf2	Fn3k	4930455F23Rik	Nek5	Tmem107	Gng8	Prr15		
Gdap111	Mreg	Me1	Hebp2	Scg3	Slc24a3	Colq	Gnacr2 <sup>a</sup>	Cartpt	Ptplad1	Htr3a	Lrrc18		
Snap25	Dscam1l	Cdkl2	Emb	Sncg	S100a13	B3gnt4	AI428936	Lrrq1	Slc9a9	Mcoln3	Mlc1		
Hevw1	Chga	Cetn2	Klh132	Dll4	Paqr9	Cdh23 <sup>a</sup>	Lrrc30	Ccdc135	Tmcc2	4432412L15Rik	Spag16		
Mycl1	Mgat5b	Fam49a	Stac	Rem1	Defb25	Bbs1	Car7	Agbl2	Nbas	Pftk2	Dnahc10		
Six1	1500001A10Rik	Pak3	Sq5	2310076L09Rik	Cpeb4	Myl3	Tmem179	D130043K22Rik	Gm705	B3galt5	Dmkn		
Brsk1	Gdap1	Nme5	Hspa2	Hist2h3c2	Ocm <sup>a</sup>	Tmie <sup>a</sup>	Pcsk9	1700001L19Rik	Sh2d4b	Dnase1	Trdn		
Ano3	Trim36	Efcab10	Trappc2	Ccdc92	3110006E14Rik	6430571L13Rik	Ptpn3	Mapk15	Card10	Art1			
Cips	Chrn9 <sup>a</sup>	1700016K19Rik	Ap1m2	Trim71	Cldn14	Rip12	Ppp1r14d	Hydin	Rab25	Plcd2	Cdc33		
Glt28d2	Rasd2	Ttc29	Atp10d	Sall1	Trnp1	Maneal	4930470P17Rik	Krt7	Tmem8				
Phtf2	Jag2 <sup>a</sup>	Slc8a2	Galnt13	Zfp697	Tmrrss6	Tppp	Mslnl	Lrrc6	Dlg2	Tpo			
Lnx2	Dfnb59	Mif1	BC030867	Ly6h	Atp1b1	Prrt3	D7Erd443e	Scn11a	1700001C02Rik	2300009A05Rik			
Nefl	Skp1a	Elmod1 <sup>a</sup>	Usp46	Mtap2	Nme7	Dlgap3	Zfp365	Necab1	Cabp2	2310021H06Rik			
Atp2b2	2310046K01Rik	Gm904	Arhgdig	Synj2	Srd5a1	Iqcg	Pclo	Plekhf2	Cpe	D630023F18Rik			
Pvalb <sup>a</sup>	Atoh1 <sup>a</sup>	1700027A23Rik	Cacnb2	Rgs11	Ablim3	Lrrc56	Spef2	Mak	Dynll2	Dbpht2			
Oscp1	4932411E22Rik	Gm1060	Kcnb1	Tcte2	Atp2a3	Gpx2	Dnaic2	Iqub		Gm879			

Genes near each other in a column have similar expression patterns during development. <sup>a</sup>Genes well known in the inner ear. <sup>b</sup>Genes validated here by ISH or immunostaining (Figs. 6 and 7).

**Table 2.** Genes expressed by surrounding cells as shown in Fig. 6

Sgms2	Esam	Birc3	Etk3	Il16	Sntb2	Dse	Vwa5a	Tgfb1i1	Slc16a4	Fabp7	Sfrp4	Gper	Ppp1r1b	Agt	Sh3pxd2b
Tspo	Plod1	Tek	Tspan9	Ptgfr	Fbn2	Fzd1	Dcn	Kctd12b	Tor3a	Rasa3	Cldn19	Ccd106	Casp12	Htra3	Aebp1
Il118	Anpep	Gm6041	Dclk1	Cd68	Fstl1	Notch2 <sup>a</sup>	Dmd	Prrg3	Angptl1	Knk5	Itga7	Em13	Cd79a	Notum	B1vrb
Nt5e	Pdlim2	Cdh5	Lox	Parp9	Tnfrsf19	Lypd6	Plp1	St3gal6	Fgrf4	Megf6	Filip1	B3gnt9	Egf18	Ltpb4	Actg2
Sidt1	Plekho2	Nrn1	Ifitm2	Slc12a4	Atp10a	Prrx1	Fam181b	Gng12	9030625A04Rik	Itga1	Gpr37l1	A730069N07Rik	Sat1	Lrtm1	Wnk4
Gbp4	Cd52	C630043F03Rik	Ath11	Fam176b	Rerg	Cgn1	Tgfb3	Snx7	Mpp1	Nes	Il1b	Slc27a6	Sfrp5	Angptl2	Pde8a
4931408A02Rik	Arhgap12	Sulf1	Lgals1	Gstt1	1110021L09Rik	Tns3	Col6a1	Sh3bp5	Ahr	Bcl2l12	Stfa2l1	Junb	P2rx7	Wtip	Crip1
Copz2	Escr	Tcfap2a	Gabrb2	Abca1	H19	Fbln2	Gas2l3	Mpp6	Cria3	Igsf10	Fpr2	Sorbs3	Gatm	Lgals3	Cpz
Cybb	Srp2	Reps2	Vstm2a	A2m	Atp1b3	Svep1	Fosf2	Ephb4	Gucy1a3	Gadd45b	Steap4	B2m	Scn7a	Cd53	Ehd2
Npnt	Grn	Fbn1	Lhfp	Trf	Ifngr1	Cyfip1	Cdh19	Tbcl1d2b	Lef1	Wdr86	Cd36	Irfl	Col15a1	Igfbp7	Igfbp6
Tagln	Lbp	Hs3st1	Itgb5	Col4a5	Mbnl2	Tax1bp3	Hspg2	Kank2	Met	Icosl	Cdkn2c	Ctsk	Mag	Ly86	Ccr2
Fam55b	Alox5ap	Rbpms	Samd4	Tmem119	Gna1	Tead1	Lamc1	Zcchc24	Camk1d	Tcrg1	Slc30a10	Otpn	Mbp	Tnfrsf11a	Nlgn1
Rin1	Lamb2	Plekhh2	Cpne2	Tspan18	Itgb1	Gng2	Sdc2	Msn	Prkcb	Tlr4	Rab38	Ptprc	BC100530	Gab3	Mmp25
Fam101a	Myl9	Slc31f1	Edhra	Sat2	Ank2	Rsu1	Mmp2	Wrm	BC057170	Rhbd1f1	Plac8	Tnfrsf11b	Stfa1	Klf15	Pdgfra
Rgs10	Pxn	Zfp703	Moxd1	Slt5a1	Slc16a1	Cnn2	Tmem45a	B4galnt6	Sgc	Arhgef6	Pon3	Bcl6	Emr1	Lyz1	Paps2
Alas2	Adcy6	Rbp1	Fmn3	Lcp2	Gpm6b	Bmp5	Hsd17b11	D16Ert472e	Finc	Bag3	Rassf5	Tcf15	S100a8	Abca8b	Mt2
Hemgn	Rtnk	A430107013Rik	Npy	Scar2	Man1c1	Kdel2	Rhoc	Pik3ip1	Anxa3	Kcnab3	Sox8	Tmprss5	S100a9	Plek	Susd5
Slc4a1	Ctsz	Entpd1	Dbi	Ramp2	Elov15	Mfap2	Atp1a2	Cnrip1	Fli1	Crl2	Angpt2	Lair1	Txnip	Aldh1a1	Tenc1
Ctse	Elovl1	Slc1a3	Itih5	Rnf130	Cytob	Eng	Col9a3	Tnks1bp1	Gpr177	Col13a1	Baiap2	Pygm	Cp	Kifc3	Fhod1
Gypa	C130074G19Rik	Nalcn	Bace2	Fgf2r	Cd200	Arap3	Cytip	St8sia1	Pkd2	Cd48	Klhdc7a	Myrip	4930539E08Rik	Ppargc1a	
Irfl8	Ndrq2	Rsd2	Col8a1	Rhou	Epb4_112	Pou3f4 <sup>a</sup>	Trim30	Slc5a7	Cdh10	C1qtnf1	Lst1	Ccl6	Enpp1	Ofm1	Arhgap30
Osbp15	Depdc6	Gpm6a	Kank4	Ppp1r14c	9030420J04Rik	Col12a1	Ctss	Prdm1	Nmi	Col24a1	Slc7a7	Msr1	Abca8a	Cox6b2	E130203B14Rik
Stard8	Arhgap19	Cobll1	Tmem176a	Cav2	Cnn3	Lpp	Serpinb1a	Twist2	Rnf43	Cxcl1	Stk17b	Fcrls	Csar1	Ggct	Cyth4
Slc43a3	Ch11	Gbp6	Arhgef10	Scd1	Cpne3	Epb4_111	Lyz2	Gpr88	Sertad4	S1pr2	Adam23	Tnmd	Inpp5d	Hexb	Fcgr4
Tagln2	Stat6	Dgka	Capn1	Kdelr3	Tcf7	Sema5a	Cd3	Rnase4	Trpc3	Large	Matn2	Barres2	C1qtnf2	Megf9	Stab1
Git1	Sema3b	Mtrm10	Fkbp7	Nek6	Akr1b8	Igf2	Cd4	Cd83	Tmem100	Ndp	Cts1	Plxn3b	Kcnai1	Car11	Gpr183
Gpx7	Stat5a	Mst46c	Fkbp14	Foxc2	Trp16	Cldn11	Cipt1	Emp2	Edar	Gria4	Il1trap	Gm525	Prx	Cd44	Klk8
Tnfrsf1a	Islr	Stxbp6	Nqo1	9430020K01Rik	Bgn	Adamts1	Glrb	Rgs5	Gm12824	Itga6	Aatk	Itgb2	Wnt6	Rarg	Rps6ka4
Aspn	Pld2	Mpeg1	Luzp2	Gdf10	Gata2	Fbln1	Sepp1	Rcsd1	Amot1	Stampb1	Stard5	I34	Cd14	Fam105a	Slc16a13
Gcom1	Rcn3	Megf10	M6prbp1	Ddr2	Lats2	Reck	Ranbp3l	9230105E10Rik	Smarc2	Cntnap4	Mfsd7c	Sod3	Nfkbid	Lgi1	Cfp
Pip5k1b	Smo	Cpm	Ar15c	Tgfb1	Iggap1	Emp1	Hbeaf	Col5a1	Adams5	Musn1	Gje1	Piwil1	Gm5483	Fmo1	Prxx2
Sncapj	Rhod	Slc2a1b	Kif10	Aard	Ets1	Arhgap29	Pcc1	Enpep	Rftn1	Tie1	Fyb	Khr1a	Slc4a10	Lrtm2	Abcd1
Cyp2d22	Cd248	Slc2a10	Sostdc1	Fam114a1	Col5a2	Zic2	Gem	Ppfibp1	Kcnj8	Chrd	Ifl27l1	Dusp15	Abhd3	Reln	Cited1
2610204M08Rik	Cercam	Klf6	Gfra2	Serpinf1	Rob12	Col23a1	Maf	Bambi	Trim12	Itga8	Kcnrg	Vwa1	Pmp2	Fam19a1	Fxyd5
Fads3	Nudt19	S100a16	Ldb2	Rgs2	Igfbp4	2810055F11Rik	Wnt5a	Gng11	Edn3	Sh3d19	Prkcdbp	Cdc7	Mal	Atp10b	Lcat
F3	Mmp15	Kn6a	Postn	Timp3	Axl	Cyp1b1	Zfp3612	Stard13	Hbb-2	Hspb1	Tropob	BC064033	Kenj10	Chrm1	Omd
Vat11	Mtpd7d1	Grik2	Aldh1a2	Ctrp	Tspan7	Cipy4	Jam3	Sertad1	Kcn3	Tcea3	Rit2	M5a47	Pllp	Gm106	
Amigo2	Oaf	Tiam1	Scara5	Col1a2	Itm2a	Rbpm52	Npl	Drp2	Plekhf1	Igtp	Nr4a2	C1qc	Itgb3	Metrn	
Fgf14	Seprn1	Pdpn	Palmd	Otor	Cagap	Arhgap28	Lama4	Tpcn1	Adcy4	Tmem150	Xlr	Ccl2	Mt1	Il15	
Slc40a1	Csrp2	Fmn2	Chst1	Ogn	Lims1	Chd3	Parva	ler3	Igta5	Igtp1	Dusp1	Entpd2	Csgalnact1	Slc26a11	
Thr3	Npc2	Fyn	Col27a1	Vcam1	Nrp1	Mmp11	Col4a6	Fcer1g	Cdc42ep1	Ctnn3	Jdp2	Gahrn6	Mrc1	Trp63	
Hmgcs2	Zfp456	Cacna1e	Icam1	Ednrb	Wwtr1	Pmp1f	Arsb	Tmem195	Cspg4	Grb14	Rxfp3	Bc2a1b	Ms4a6d	Cd74	
1110032E23Rik	Ptprs	Fat1	Igf1	Add3	Col6a2	Mlx	Hlf	Itgb1l	Apodd1	Ltpb2	Csmp1	Tfp12	Samsn1	Cla2b	
Lonrf3	Gpr137b	Fat4	Slco1c1	Gypc	Pls3	Pdgfrb	Lpar1	Apoe	Sardh	Sparc1	Nfkbiaz	Dmp1	Gpr65	Tmc6	
Ptgr1	2010002N04Rik	Pldx2	A930038C07Rik	Aldh2	Nid1	Acsf2	Cal8a2	Srgn	Arhgap15	Rin3	Zfp36	Gcg	Slc3a6a2	Efna1	
Pea15a	Cyth3	Lmo2	Anxa1	Igmap6	Egflam	Sh3tc2	Ahnak	Ctsh	Cyba	Clip2	Fbln5	C3ar1	Tmem71	H2-Aa	
Tmem176b	Rhog	1810055G02Rik	Mettl7a1	Thbd	Col4a1	Enpp2	Pcoke	Pmp22	Emilin1	Il10ra	Lama2	Hnmrt	Lirb4	Car1	
Car3	Capsn1	Eprd1	Pltp	Fkbp10	Dox3l	Cal901	Cal14a1	Fcgtr	Hmha1	Ac03	Egr2	A33049M08Rik	Sard1	Napt1	
Htr4	Fxyd6	Tgm2	S100a4	Lepre1	Slt2	Serpine2	Rab32	Timp2	Cd97	Lynx1	Pik3cg	Slc44a1	Slc7a8	Dct	
Slc24a6	Paqr4	Ccdc102a	Serpibn9	Acss1	Ppic	Naadal2	BC013529	Sparc	Tmem37	Cd37	Sla	Nr4a1	Thbs2	Ephb6	
Cebpa	Anxa2	Tmem204	Apod	Ctdsp1	Serpinh1	5033414K04Rik	Cxd12	Mpz	Mum11	Slc25a45	Prelp	Cxcl10	Nupr1	Nudt13	
Pdgfrl	Fxyd1	Emid2	Cxcl16	Lrp1	Kctd12	Col11a1	Maob	Sult1a1	2900092D14Rik	Dock2	Zc3hav1	Abca6	Slc13a5	Dock5	
Col16a1	Galnt4	Rftm2	Mxra8	Emp3	Tbx18	Gnb16	Trpm4	Nap1l5	Pou3f3	Runx2	Itgav	Ptn	Paqrl6	Il11ra1	
Cry1	C630028N24Rik	Mgst1	Cav1	Mgp	Ckap4	Spt7	Pmepa1	Itga11	Lrrtm4	Ddn	Col1a1	Cyp2j9	4632428N05Rik	Gjb2a	
Lgi4	Esyt2	Nrf2f	Col4a2	Col2a1	Itpr1pl2	Aldh3a1	S100a11	Abcg2	Pdzd2	2010005H15Rik	Jam2	Emr4	Car14	Slc6a1	
Serp1	Mdf1c	Scara3	Wif1	Ifitm3	Rhoj	Selenbp1	4933428G20Rik	Leprel2	Spats2l	Rbp4	Arhgap6	Adra2a	Adams2	Cmbl	
Col5a3	Ttc23	Wisp1	Acot1	Nbl1	Cald1	Adcy7	Adams12	Epas1	Fndc3b	Apoda4	Dpyd	Cebpd	Dio2	Emid1	
Bcas1	Vgll4	Daam2	Prss12	Gnb4	Cntm3	Kcnk2	Tln1	Runx2	Tnfrsf1b	Gstt3	Ptn	Nr3c2	Tm4sf1		
Ndr1g	Foxa4	Iftm1	Capn5	Lyn	Antxr1	Oat	Cd302	Afap111	Acadl	Fgbp1	Slc10a3	Adm	Aox1	BC017612	
Lrrc4c	Apobec3	Tnfaip6	Dhrs2	Rab31	Dab2	Afap112	Tgfb3	Mterfd2	Etv1	Slco1a4	A4galt	Atf3	Mpa2l	Phlbd1	
Fzd5	Bmp1	Nov	Plekha4	Lox13	Kif1c	Gulp1	Jun	Ltbr	Ankrd27	Fcgr3	Ccd80	Parp14	Gbp10	S1pr1	
Nav3	Trim26	Efemp1	Hmox1	S1pr3	Slc1a2	Sox10 <sup>a</sup>	Nod1	Hpgd	Id3 <sup>b</sup>	Clec4a2	Foxd3	C030030A07Rik	Cts	Ism1	
Rasgrp2	Dchs1	Emcr <sup>b</sup>	Nid2	Ctdsp2	Abca9	Slc16a9	Trpm5	Plxnd1	Sumf2	Gpr34	Phlda1	Pou3f1	Ly6a	Lect1	
Syk	Acot9	Ptms	Coch	Tim1	Flna	Spx	Rob34	Lcp1	Vasn	Ccr5	Marf6	2310046A06Rik	Flt3l	Hic1	
Gstt2	Nfatc4	Lipa	Aspa	Tgff1	Tle1	Dhh	Cd38	Fam109b	P2ry1	Clec4a3	Eln	Stfa2	Mybpc1	Kbtbd11	
Ir4	Mobkl2a	Lum	Lamb1-1	Tmem132c	Agr2	Ctsc	St3gal4	Rras	Pros1	Adams20	Lrrc4b	Stfa3	Nkd1	Car2	
Hbb-b1	Plp2	Heph	Nr3c1	Capn6	Yap1	Hfe	Gpr124	Cpxm1	Jub	Csf1r	Pde1a	Cfh	Pamr1	Casq1	
Arhgef1	Bnc2	Plk2	Pear1	Twist1	Npr3	Itgb8	Mitf	Uap111	Ldfr	C1qa	Rel	Cntn6	Pdhd9	Ephb3	
Gpx8	Frk	Crispld1	Ptpn14	Crybg3	Tnfaip8	Ptpre	Clist14	Cyr61	Fgd5	Tlr7	Ly96	Cxcl2	Stear3	Zawpw1	

Genes near each other in a column have similar expression patterns during development. <sup>a</sup>Genes well known in the inner ear. <sup>b</sup>Genes validated here by ISH.

similarly involved in ion transport. The low number of reads in cochlear SCs, in contrast to the conspicuous expression in the stria vascularis, is probably because the stria vascularis was not included in the sensory epithelium dissected for FACS. We also used immunocytochemistry to validate predicted expression and to confirm translation of selected genes. *Lmod3* en-

codes leiomodin 3, an actin-filament nucleator (Chereau et al., 2008; Campellone and Welch, 2010; Nanda and Miano, 2012). It was predicted from HTS data to be expressed only in HCs of cochlea but not utricle, and primarily at the later two developmental stages. With antibody labeling, we found strong leiomodin 3 labeling of cochlear outer but not inner hair cells at P6, and

little or no label in the utricle, consistent with *in situ* hybridization (Figs. 7D, 8A). A closely related gene, *Lmod1*, was apparently expressed in all HCs; it was found in the embryonic and postnatal HC cluster (Fig. 6A, Table 1). By antibody label we found it throughout the cytoplasm of all HCs of the cochlea and utricle, but not SCs, as predicted by HTS (Fig. 8B).

Similarly, *Ldb3* encodes the cardiac muscle protein LIM-domain-binding 3 (LDB3/ZASP/Cypher), which links  $\alpha$ -actinin-2 to PKC (Zhou et al., 1999). HTS counts predict expression only in HCs, and more in utricular than cochlear HCs. Consistent with HTS data, we found sparse LDB3 labeling in cochlear IHCs and strong labeling in vestibular HCs, with striking localization at the circumferential actin bands of the zonula adherens (Fig. 8C). Although a limited number of genes was tested, immunocytochemistry suggests that gene expression at the mRNA level generally reflects protein expression.

#### Biological process changes with age

HCs in both cochlea and utricle undergo a striking differentiation between E16 and P7. The development of the cochlea is not perfectly correlated with development of the utricle: the utricle gains mechanosensitivity by E17, whereas the cochlea is delayed until P2, and hair bundles have all formed in cochlea by P2, whereas some continue to develop in utricle for 2 weeks. Even within the cochlea, development progresses from base to apex over  $\sim$ 2 d. However the broad patterns of expression may be revealed by ages separated by 3–4 d. We generated four lists of genes that are preferentially expressed in all HCs at E16, P0, P4, or P7. To investigate the biological processes associated with HC development, we used the Database for Annotation, Visualization and Integrated Discovery (DAVID) for functional annotation of these genes (Huang da et al., 2009a, b). DAVID uses the Gene Ontology classifications of associated genes with biological processes, and then calculates which processes are strongly represented in a specific gene list.

Figure 9 represents the degree of enrichment for 43 of the most represented processes, and how enrichment changes with age. E16 HCs mostly expressed genes related to morphogenesis, differentiation, and development, reflecting the transition to a HC phenotype. P0 and P4 HCs continued to express genes associated with differentiation, but sensory and inner ear categories were more highly represented.

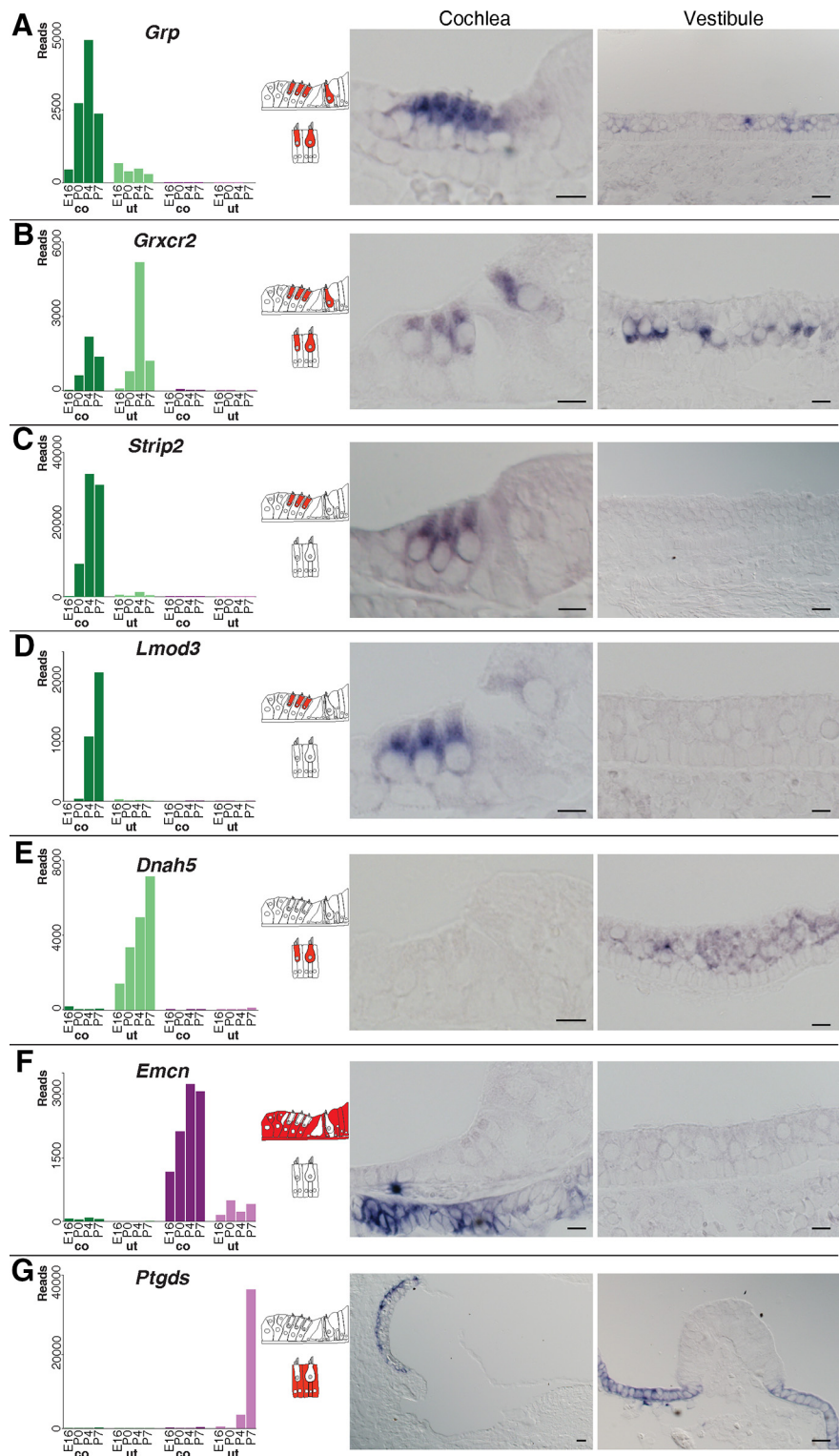


**Figure 7.** Validation by *in situ* hybridization of cell specificity predicted from hierarchical clustering. Shown for each gene are the normalized HTS read counts for each condition (left), a schematic of the predicted cell specificity based on these counts (middle), and *in situ* hybridization in cochlear and vestibular sensory epithelia (right). Scale bars: 20  $\mu$ m. **A**, *Grp* was expressed in both cochlear and saccular hair cells at E18. **B**, *Grxcr2* was expressed in both cochlear and utricular hair cells at P6. **C**, **D**, *Strip2* and *Lmod3* were detected only in P6 OHCs. **E**, *Dnah5* expression was restricted to utricular hair cells at P6. **F**, *Emcn*, predicted to be in cochlear surrounding cells, was found mostly in basilar membrane at P6. **G**, *Ptgds*, predicted to be mainly in vestibular surrounding cells, was found adjacent to the sensory epithelium of the ampulla but also in the stria vascularis of the cochlea at E18. Co, cochlea; ut, utricle.

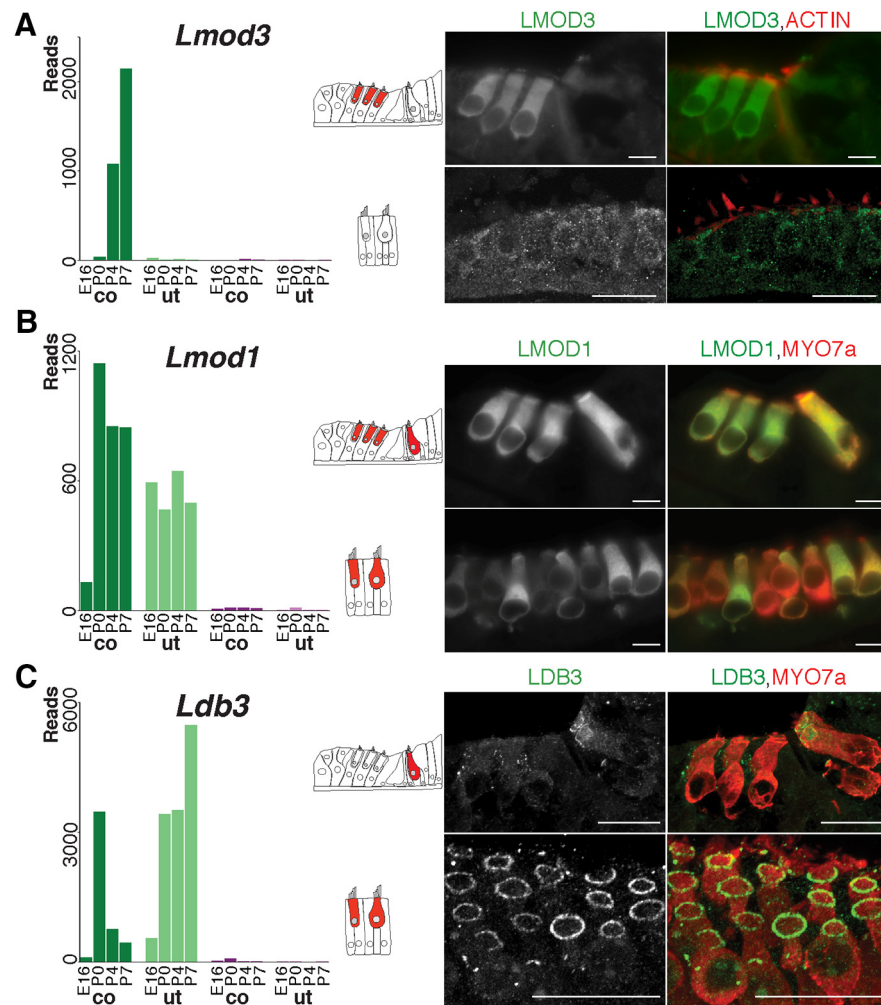


**Figure 8.** Validation by immunocytochemistry of predicted cell specificity at P6. Normalized HTS read counts for each condition, predicted cell specificity, and antibody labeling in cochlear and vestibular sensory epithelia. Scale bars: 20  $\mu$ m. **A**, *Lmod3* was found mostly in cochlear but not utricular hair cells; within the cochlea, it was expressed mainly in OHCs. **B**, *Lmod1* was found in all cochlear and utricular hair cells and was located throughout the cell bodies. **C**, *Ldb3* was found in cochlear and utricular hair cells; in the cochlea, it was expressed mainly in IHCs. *LDB3* immunoreactivity was localized to the zonula adherens region. Co, cochlea; ut, utricle.

P7 HCs were no longer enriched in morphogenesis genes, but showed much more representation of cell signaling and synaptic genes, consistent with a mature phenotype. Although P4 HCs are largely mature in mechanosensation, these data reveal further differentiation of function between P4 and P7, especially as HCs connect to the brain.

## Discussion

### Isolation of HCs

Biochemical and molecular genetic studies of the HC proteome have been difficult because HCs are embedded in a sensory epithelium that includes a variety of other cell types. Biochemical characterization of one organelle—the stereocilium—has been achieved by mechanical harvesting of hair bundles (Shepherd et al., 1989; Gillespie and Hudspeth, 1991; J.B. Shin et al., 2010), but the rest of the HC has been hard to purify. A zebrafish transgenic line expressing GFP in hair cells (*Tg(pou4f3:GAP-GFP)*) was used to purify precursors of lateral line HC for characterizing gene expression during HC regeneration (Steiner et al., 2014), looking at earlier stages of cell-fate determination. Hertzano et al. (2011) used the endogenous cell-surface markers CD326 (*Ep-*

*cam*) and CD49f (*Itga6*) to separate the sensory epithelial cells from nonsensory cells. Our data show, however, that these markers are not specific to HCs. In this study, we used FACS of cells from a transgenic mouse line (*Pou4f3-Islet-eGFP*) to separately purify HCs and SCs of the cochlea and the utricle. Based on the relative abundance of selected mRNAs from brightly fluorescent and nonfluorescent cells, we estimate that the samples were >99% pure.

Sorting based on *Pou4f3* expression provides higher purity than with some other HC markers such as *Atoh1*. For instance, we and others have FACS-purified HC from the *Tg(Atoh1-GFP)* mouse line (M. Huang and Z.-Y. Chen, unpublished observations; Sinkkonen et al., 2011). In those experiments we found significant contamination from supporting cells, a likely consequence of the expression of *Atoh1* in the common progenitors of HC and supporting cells (Yang et al., 2010; Driver et al., 2013). *Gfi1* is strongly expressed by HCs, but we found it to be expressed as well by a few other cell types in the cochlea (data not shown). *Pou4f3* expression is limited to HCs, so its promoter is a better driver of HC-specific markers (Huang et al., 2011; Masuda et al., 2011).

Picking single cells with visual guidance is another way to achieve high purity, as HCs are morphologically distinguishable from surrounding cells. In this way, Liu et al. (2014) investigated gene expression in adult IHCs and in OHCs, but were not able to compare them to SCs (Liu et al., 2014). In the top 200 genes they found expressed in IHCs or OHCs, we found that only 42 or 50, respectively, were enriched by more than twofold in the cochlea at P7. For instance, they found expression of the ion channel genes *Trpm3* and *Trpm7* in HCs, as we did, but these genes are expressed even more highly in SCs. Comparing HC expression with SCs, at different ages, complements such studies and gives additional insight into function.

### Advantages of RNA-Seq

We used RNA-Seq to generate an unbiased dataset of HC and SC mRNAs. In other studies, a pool of 30–100 cells was sufficient to obtain high-resolution transcriptomes with RNA-Seq (Marinov et al., 2014), so our dataset, with a minimum of 1120 sorted cells (Fig. 1D), is expected to accurately represent HC gene expression. RNA-Seq has a much higher dynamic range than the microarrays used in our previous studies (Scheffer et al., 2007a, b), with read counts varying over a millionfold in these samples. Moreover, a significant number of genes are not represented on microarrays or have sequence errors. For instance, RNA-Seq data led us to study the *Xirp2* gene (Scheffer et al., 2015), but no probe sets corresponding to *Xirp2* are included in the Affymetrix Mouse GeneChips MG-U74v2 or MOE430 that we used previously (Scheffer et al., 2007b). Although newer microarrays are more

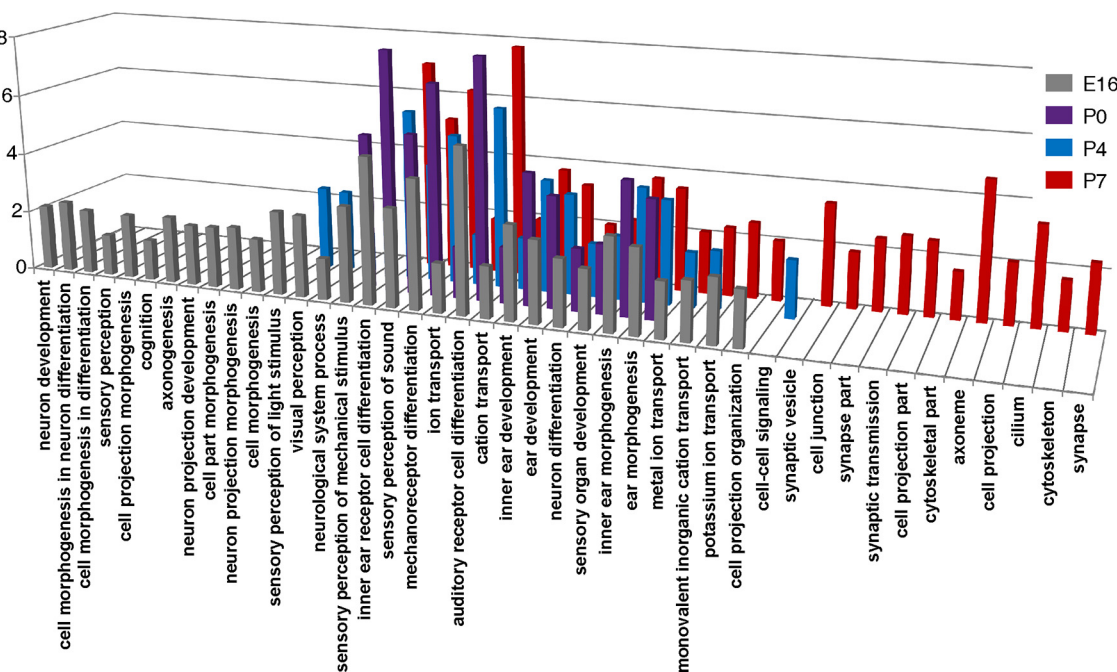


**Figure 9.** Enrichment of gene ontology categories expressed by HCs at E16 (gray), P0 (purple), P4 (blue), and P7 (red). The y-axis represents the enrichment (observed number of genes/expected).

representative, they are still limited to known transcript isoforms, are unable to detect transcripts expressed at low levels, are saturated for highly expressed transcripts, and are difficult to use for cross-platform analysis. RNA-Seq data may be reanalyzed with data from different studies or with new reference sequences to generate new insights. While RNA-Seq data do not replace existing microarray-generated transcriptomic data, the miniaturization of RNA-Seq library preparation, the high multiplexibility with DNA barcodes, the ability to use single cells (Shalek et al., 2014), and the striking decline in sequencing costs all suggest that RNA-Seq should be the method of choice for transcript quantification and identification.

### SHIELD database

We compiled these expression data in the Shared Harvard Inner Ear Laboratory Database (SHIELD; <https://shield.hms.harvard.edu>). It includes similar expression data from other laboratories (Lu et al., 2011; Shin et al., 2013; Kwan et al., 2015) and provides links for each gene to a variety of other databases.

### Sorting by hierarchical analysis of gene expression

To understand the development and differentiation of HC, we performed RNA-Seq of HC mRNA at various developmental stages. These data can be sorted or clustered in a variety of ways to identify genes that may be involved in particular functions. We began with a hierarchical clustering that groups genes based on their expression levels in the 16 conditions. We were able to identify genes that are upregulated during development of mechanosensitivity (E16 compared with P0 in the utricle and P0 compared with P4 in the cochlea). Many such genes are known to be essential for HC function (Fig. 6A, B), and these include the following: *Tmc1*, *Tmc2*, *Pcdh15*, *Cdh23*, *Lhfp15*, *Myo15*, *Tmie*, and *Fscn2*. It is likely that many more genes important for mechanotransduction are among this subset.

Another cluster contained genes that are highly expressed in cochlear HCs but less so in utricular HCs (Fig. 6C). Because the

cochlear sample is dominated by OHCs, many genes enriched in cochlea relative to utricle may participate in functions unique to OHCs. With *in situ* hybridization or specific antibodies, we validated the restricted expression in OHCs of two such genes, *Lmod3* and *Strip2* (Figs. 6C,D, 7A). The STRIP2 protein is associated with cortical F-actin bundles and cell–cell adhesion (Goudreault et al., 2009; Bai et al., 2011) and may participate in the OHC cortical lattice. *Slc26a5*, *Strip2*, and *Lmod3* were consistently found in the 222 genes enriched in cochlear HCs (Fig. 2D). Our comparison of cochlear and utricular HCs is not as direct as that of Liu et al. (2014) for determining IHC and OHC differences, but has the advantages of much greater dynamic range and an understanding of changes in expression during development.

A third cluster is expressed in HCs, but more highly in utricle than cochlea (Fig. 6D). Some of these encode proteins associated with microtubule-based cilia; they could be components of the kinocilia, which are present in utricle but absent in mature cochlea.

Some closely related genes have very different expression patterns in the inner ear, reflecting distinct function even within one cell type such as HCs. For instance, the leiomodins, *Lmod1* and *Lmod3* (Fig. 8), are differentially expressed: *Lmod1* is expressed in all HCs of the inner ear, throughout development, whereas *Lmod3* is restricted to the OHC, and only after P0.

It is important to recognize the limitations of such comparisons. In this analysis, genes highly enriched in HCs are enriched only relative to SCs. They might be highly expressed in related cell types such as central neurons, and not unique to HCs. Similarly, genes expressed in both HCs and SCs might, nevertheless, be exclusive to inner ear sensory epithelia and appear nowhere else in the body. Comparison to expression databases from other tissues can help illuminate the possible functions of a gene.

Finally, genes expressed in other cochlear cell types and important for other aspects of cochlear function could be identified in the same way, limited only by the availability and specificity of

mouse lines expressing a fluorescent tag in certain cells of the inner ear.

## Deafness

These data, presented in the SHIELD database, have already helped identify a new Usher syndrome gene, *CIB2* (Riazuddin et al., 2012), and helped confirm the HC expression of *Kir2*, an inwardly rectifying potassium channel protein (Levin and Holt, 2012). One of the genes most highly enriched in our HC data is *Grxcr2*, and mutations in human *GRXCR2* were recently found to cause recessive hearing loss (Imtiaz et al., 2014). Another highly enriched gene is *XIRP2*; in related work we found *XIRP2* to be associated with the stereocilia and cuticular plates of HCs, and to cause progressive stereocilia disorganization when absent (Scheffer et al., 2015). We expect that these expression data will aid in the discovery of additional human deafness genes. In addition, deafness is not always associated with vestibular dysfunction, and indeed we found many genes enriched in just cochlea or utricle. Differential expression data should aid in understanding the etiology of complex inner ear disorders.

In summary, we performed the first comprehensive gene expression study specific for vestibular and cochlear HCs during mouse development. The public database generated is a powerful tool for discovering and understanding proteins involved in HC function. We anticipate these data will lead to the discovery of new genes important for HC mechanotransduction and new deafness genes in mouse and human.

## References

- Anders S, Huber W (2010) Differential expression analysis for sequence count data. *Genome Biol* 11:R106. CrossRef Medline
- Asmann YW, Klee EW, Thompson EA, Perez EA, Middha S, Oberg AL, Therneau TM, Smith DI, Poland GA, Wieben ED, Kocher JP (2009) 3' tag digital gene expression profiling of human brain and universal reference RNA using Illumina Genome Analyzer. *BMC Genomics* 10:531. CrossRef Medline
- Bai SW, Herrera-Abreu MT, Rohn JL, Racine V, Tajadura V, Suryavanshi N, Bechtel S, Wiemann S, Baum B, Ridley AJ (2011) Identification and characterization of a set of conserved and new regulators of cytoskeletal organization, cell morphology and migration. *BMC Biol* 9:54. CrossRef Medline
- Beckers A, Alten L, Viebahn C, Andre P, Gossler A (2007) The mouse homeobox gene *Noto* regulates node morphogenesis, notochordal ciliogenesis, and left-right patterning. *Proc Natl Acad Sci U S A* 104:15765–15770. CrossRef Medline
- Bermingham NA, Hassan BA, Price SD, Vollrath MA, Ben-Arie N, Eatock RA, Bellen HJ, Lysakowski A, Zoghbi HY (1999) *Math1*: an essential gene for the generation of inner ear hair cells. *Science* 284:1837–1841. CrossRef Medline
- Bermingham-McDonogh O, Oesterle EC, Stone JS, Hume CR, Huynh HM, Hayashi T (2006) Expression of *Prox1* during mouse cochlear development. *J Comp Neurol* 496:172–186. CrossRef Medline
- Campellone KG, Welch MD (2010) A nucleator arms race: cellular control of actin assembly. *Nat Rev Mol Cell Biol* 11:237–251. CrossRef Medline
- Carlisle FA, Steel KP, Lewis MA (2012) Specific expression of *Kcnal10*, *Pxn* and *Odf2* in the organ of Corti. *Gene Expr Patterns* 12:172–179. CrossRef Medline
- Chen P, Segil N (1999) p27(Kip1) links cell proliferation to morphogenesis in the developing organ of Corti. *Development* 126:1581–1590. Medline
- Chereau D, Boczkowska M, Skwarek-Maruszewska A, Fujiwara I, Hayes DB, Rebowski G, Lappalainen P, Pollard TD, Dominguez R (2008) Leiomodin is an actin filament nucleator in muscle cells. *Science* 320:239–243. CrossRef Medline
- Cotanche DA, Kaiser CL (2010) Hair cell fate decisions in cochlear development and regeneration. *Hear Res* 266:18–25. CrossRef Medline
- Driver EC, Sillers L, Coate TM, Rose MF, Kelley MW (2013) The *Atoh1*-lineage gives rise to hair cells and supporting cells within the mammalian cochlea. *Dev Biol* 376:86–98. CrossRef Medline
- Dumont RA, Lins U, Filoteo AG, Penniston JT, Kachar B, Gillespie PG (2001) Plasma membrane Ca<sup>2+</sup>-ATPase isoform 2a is the PMCA of hair bundles. *J Neurosci* 21:5066–5078. Medline
- Géléc GS, Holt JR (2003) Developmental acquisition of sensory transduction in hair cells of the mouse inner ear. *Nat Neurosci* 6:1019–1020. CrossRef Ref Medline
- Géléc GS, Holt JR (2014) Sound strategies for hearing restoration. *Science* 344:1241062. CrossRef Medline
- Gillespie PG, Hudspeth AJ (1991) High-purity isolation of bullfrog hair bundles and subcellular and topological localization of constituent proteins. *J Cell Biol* 112:625–640. CrossRef Medline
- Golub TR, Slonim DK, Tamayo P, Huard C, Gaasenbeek M, Mesirov JP, Coller H, Loh ML, Downing JR, Caligiuri MA, Bloomfield CD, Lander ES (1999) Molecular classification of cancer: class discovery and class prediction by gene expression monitoring. *Science* 286:531–537. CrossRef Medline
- Goudreault M, D'Ambrosio LM, Kean MJ, Mullin MJ, Larsen BG, Sanchez A, Chaudhry S, Chen GI, Sicheri F, Nesvizhskii AI, Aebersold R, Raught B, Gingras AC (2009) A PP2A phosphatase high density interaction network identifies a novel striatin-interacting phosphatase and kinase complex linked to the cerebral cavernous malformation 3 (CCM3) protein. *Mol Cell Proteomics* 8:157–171. CrossRef Medline
- Groves AK (2010) The challenge of hair cell regeneration. *Exp Biol Med* 235:434–446. CrossRef Medline
- Hartman BH, Basak O, Nelson BR, Taylor V, Bermingham-McDonogh O, Reh TA (2009) *Hes5* expression in the postnatal and adult mouse inner ear and the drug-damaged cochlea. *J Assoc Res Otolaryngol* 10:321–340. CrossRef Medline
- Hertzano R, Dror AA, Montcouquiol M, Ahmed ZM, Ellsworth B, Camper S, Friedman TB, Kelley MW, Avraham KB (2007) *Lhx3*, a LIM domain transcription factor, is regulated by *Pou4f3* in the auditory but not in the vestibular system. *Eur J Neurosci* 25:999–1005. CrossRef Medline
- Hertzano R, Elkorn R, Kurima K, Morrison A, Chan SL, Sallin M, Biedlingmaier A, Darling DS, Griffith AJ, Eisenman DJ, Strome SE (2011) Cell type-specific transcriptome analysis reveals a major role for *Zeb1* and *miR-200b* in mouse inner ear morphogenesis. *PLoS Genet* 7:e1002309. CrossRef Medline
- Huang da W, Sherman BT, Lempicki RA (2009a) Bioinformatics enrichment tools: paths toward the comprehensive functional analysis of large gene lists. *Nucleic Acids Res* 37:1–13. CrossRef Medline
- Huang da W, Sherman BT, Lempicki RA (2009b) Systematic and integrative analysis of large gene lists using DAVID bioinformatics resources. *Nat Protoc* 4:44–57. CrossRef Medline
- Huang M, Sage C, Li H, Xiang M, Heller S, Chen ZY (2008) Diverse expression patterns of LIM-homeodomain transcription factors (LIM-HDs) in mammalian inner ear development. *Dev Dyn* 237:3305–3312. CrossRef Medline
- Huang M, Sage C, Tang Y, Lee SG, Petrillo M, Hinds PW, Chen ZY (2011) Overlapping and distinct pRb pathways in the mammalian auditory and vestibular organs. *Cell Cycle* 10:337–351. CrossRef Medline
- Huang M, Kantardzhieva A, Scheffer D, Liberman MC, Chen ZY (2013) Hair cell overexpression of *Islet1* reduces age-related and noise-induced hearing loss. *J Neurosci* 33:15086–15094. CrossRef Medline
- Hume CR, Bratt DL, Oesterle EC (2007) Expression of *LHX3* and *SOX2* during mouse inner ear development. *Gene Expr Patterns* 7:798–807. CrossRef Medline
- Imtiaz A, Kohrman DC, Naz S (2014) A frameshift mutation in *GRXCR2* causes recessively inherited hearing loss. *Hum Mutat* 35:618–624. CrossRef Medline
- Jones JM, Montcouquiol M, Dabdoub A, Woods C, Kelley MW (2006) Inhibitors of Differentiation and DNA Binding (Id)s Regulate *Math1* and Hair Cell Formation during the Development of the Organ of Corti. *J Neurosci* 26:550–558. CrossRef Medline
- Kawashima Y, Géléc GS, Kurima K, Labay V, Lelli A, Asai Y, Makishima T, Wu DK, Della Santina CC, Holt JR, Griffith AJ (2011) Mechanotransduction in mouse inner ear hair cells requires transmembrane channel-like genes. *J Clin Invest* 121:4796–4809. CrossRef Medline
- Keithley EM, Erkman L, Bennett T, Lou L, Ryan AF (1999) Effects of a hair cell transcription factor, *Brn-3.1*, gene deletion on homozygous and heterozygous mouse cochleas in adulthood and aging. *Hear Res* 134:71–76. CrossRef Medline
- Kwan KY, Shen J, Corey DP (2015) C-MYC transcriptionally amplifies

- SOX2 target genes to regulate self-renewal in multipotent otic progenitor cells. *Stem Cell Reports* 4:47–60. CrossRef Medline
- Lee SI, Conrad T, Jones SM, Lagziel A, Starost MF, Belyantseva IA, Friedman TB, Morell RJ (2013) A null mutation of mouse *Kcnal10* causes significant vestibular and mild hearing dysfunction. *Hear Res* 300:1–9. CrossRef Medline
- Lelli A, Asai Y, Forge A, Holt JR, Géléc GS (2009) Tonotopic gradient in the developmental acquisition of sensory transduction in outer hair cells of the mouse cochlea. *J Neurophysiol* 101:2961–2973. CrossRef Medline
- Levin ME, Holt JR (2012) The function and molecular identity of inward rectifier channels in vestibular hair cells of the mouse inner ear. *J Neurophysiol* 108:175–186. CrossRef Medline
- Liu H, Pecka JL, Zhang Q, Soukup GA, Beisel KW, He DZ (2014) Characterization of transcriptomes of cochlear inner and outer hair cells. *J Neurosci* 34:11085–11095. CrossRef Medline
- Lu CC, Appler JM, Houseman EA, Goodrich LV (2011) Developmental profiling of spiral ganglion neurons reveals insights into auditory circuit assembly. *J Neurosci* 31:10903–10918. CrossRef Medline
- Marinov GK, Williams BA, McCue K, Schroth GP, Gertz J, Myers RM, Wold BJ (2014) From single-cell to cell-pool transcriptomes: stochasticity in gene expression and RNA splicing. *Genome Res* 24:496–510. CrossRef Medline
- Masuda M, Dulon D, Pak K, Mullen LM, Li Y, Erkman L, Ryan AF (2011) Regulation of POU4F3 gene expression in hair cells by 5' DNA in mice. *Neuroscience* 197:48–64. CrossRef Medline
- Morrissy AS, Morin RD, Delaney A, Zeng T, McDonald H, Jones S, Zhao Y, Hirst M, Marra MA (2009) Next-generation tag sequencing for cancer gene expression profiling. *Genome Res* 19:1825–1835. CrossRef Medline
- Nanda V, Miano JM (2012) Leiomodin 1, a new serum response factor-dependent target gene expressed preferentially in differentiated smooth muscle cells. *J Biol Chem* 287:2459–2467. CrossRef Medline
- Peng AW, Salles FT, Pan B, Ricci AJ (2011) Integrating the biophysical and molecular mechanisms of auditory hair cell mechanotransduction. *Nat Commun* 2:523. CrossRef Medline
- Qian D, Jones C, Rzadzinska A, Mark S, Zhang X, Steel KP, Dai X, Chen P (2007) Wnt5a functions in planar cell polarity regulation in mice. *Dev Biol* 306:121–133. CrossRef Medline
- Riazuddin S, Belyantseva IA, Giese AP, Lee K, Indzhykulian AA, Nandamuri SP, Yousaf R, Sinha GP, Lee S, Terrell D, Hegde RS, Ali RA, Anwar S, Andrade-Elizondo PB, Sirmaci A, Parise LV, Basit S, Wali A, Ayub M, Ansar M, et al. (2012) Alterations of the CIB2 calcium- and integrin-binding protein cause Usher syndrome type 1J and nonsyndromic deafness DFNB48. *Nat Genet* 44:1265–1271. CrossRef Medline
- Robertson NG, Resendes BL, Lin JS, Lee C, Aster JC, Adams JC, Morton CC (2001) Inner ear localization of mRNA and protein products of COCH, mutated in the sensorineural deafness and vestibular disorder, DFNA9. *Hum Mol Genet* 10:2493–2500. CrossRef Medline
- Scheffer D, Sage C, Corey DP, Pingault V (2007a) Gene expression profiling identifies Hes6 as a transcriptional target of ATOH1 in cochlear hair cells. *FEBS Lett* 581:4651–4656. CrossRef Medline
- Scheffer D, Sage C, Plazas PV, Huang M, Wedemeyer C, Zhang DS, Chen ZY, Elgoyhen AB, Corey DP, Pingault V (2007b) The alpha1 subunit of nicotinic acetylcholine receptors in the inner ear: transcriptional regulation by ATOH1 and co-expression with the gamma subunit in hair cells. *J Neurochem* 103:2651–2664. CrossRef Medline
- Scheffer DI, Zhang D-S, Shen J, Indzhykulian A, Karavitaki KD, Xu YJ, Wang Q, Lin JJ-C, Chen Z-Y, Corey DP (2015) XIRP2, an actin-binding protein essential for inner ear hair-cell stereocilia. *Cell Rep* 10:1811–1818. CrossRef Medline
- Schimmmang T (2013) Transcription factors that control inner ear development and their potential for transdifferentiation and reprogramming. *Hear Res* 297:84–90. CrossRef Medline
- Shalek AK, Satija R, Shuga J, Trombetta JJ, Gennert D, Lu D, Chen P, Gertner RS, Gaublomme JT, Yosef N, Schwartz S, Fowler B, Weaver S, Wang J, Wang X, Ding R, Raychowdhury R, Friedman N, Hacohen N, Park H, et al. (2014) Single-cell RNA-seq reveals dynamic paracrine control of cellular variation. *Nature* 510:363–369. CrossRef Medline
- Shepherd GM, Barres BA, Corey DP (1989) “Bundle blot” purification and initial protein characterization of hair cell stereocilia. *Proc Natl Acad Sci U S A* 86:4973–4977. CrossRef Medline
- Shin JB, Longo-Guess CM, Gagnon LH, Saylor KW, Dumont RA, Spinelli KJ, Pagana JM, Wilmarth PA, David LL, Gillespie PG, Johnson KR (2010) The R109H variant of fascin-2, a developmentally regulated actin cross-linker in hair-cell stereocilia, underlies early-onset hearing loss of DBA/2J mice. *J Neurosci* 30:9683–9694. CrossRef Medline
- Shin JB, Krey JF, Hassan A, Metlagel Z, Tauscher AN, Pagana JM, Sherman NE, Jeffery ED, Spinelli KJ, Zhao H, Wilmarth PA, Choi D, David LL, Auer M, Barr-Gillespie PG (2013) Molecular architecture of the chick vestibular hair bundle. *Nat Neurosci* 16:365–374. CrossRef Medline
- Shin MJ, Lee JH, Yu DH, Kim HJ, Bae KB, Yuh HS, Kim MO, Hyun BH, Lee S, Park R, Ryoo ZY (2010) Spatiotemporal expression of tmie in the inner ear of rats during postnatal development. *Comp Med* 60:288–294. Medline
- Sinkkonen ST, Chai R, Jan TA, Hartman BH, Laske RD, Gahlen F, Sinkkonen W, Cheng AG, Oshima K, Heller S (2011) Intrinsic regenerative potential of murine cochlear supporting cells. *Sci Rep* 1:26. CrossRef Medline
- Smith RJH, Shearer AE, Hildebrand MS, Van Camp G (1993) Deafness and hereditary hearing loss overview. In: *GeneReviews(R)* (Pagon RA, Adam MP, Ardinger HH, Wallace SE, Amemiya A, Bird TD, Dolan CR, Fong CT, Smith RJH, Stephens K, eds). Seattle, WA: University of Washington.
- Steijger T, Abril JF, Engström PG, Kokociński F, Hubbard TJ, Guigó R, Harrow J, Bertone P, Consortium R (2013) Assessment of transcript reconstruction methods for RNA-seq. *Nat Methods* 10:1177–1184. CrossRef Medline
- Steiner AB, Kim T, Cabot V, Hudspeth AJ (2014) Dynamic gene expression by putative hair-cell progenitors during regeneration in the zebrafish lateral line. *Proc Natl Acad Sci U S A* 111:E1393–E1401. CrossRef Medline
- Yang H, Xie X, Deng M, Chen X, Gan L (2010) Generation and characterization of Atoh1-Cre knock-in mouse line. *Genesis* 48:407–413. CrossRef Medline
- Yoon H, Lee DJ, Kim MH, Bok J (2011) Identification of genes concordantly expressed with Atoh1 during inner ear development. *Anat Cell Biol* 44:69–78. CrossRef Medline
- Zhou Q, Ruiz-Lozano P, Martone ME, Chen J (1999) Cypher, a striated muscle-restricted PDZ and LIM domain-containing protein, binds to alpha-actinin-2 and protein kinase C. *J Biol Chem* 274:19807–19813. CrossRef Medline
- Zine A, Van De Water TR, de Ribaupierre F (2000) Notch signaling regulates the pattern of auditory hair cell differentiation in mammals. *Development* 127:3373–3383. Medline
- Zuo J (2002) Transgenic and gene targeting studies of hair cell function in mouse inner ear. *J Neurobiol* 53:286–305. CrossRef Medline